Fate-determining mechanisms in epithelial–myofibroblast transition: major inhibitory role for Smad3

András Masszi,[1] Pam Speight,[1] Emmanuel Charbonney,[1,2] Monika Lodyga,[1] Hiroyasu Nakano,[4] Katalin Szászi,[1,3] and András Kapus[1,3]

[1]Keenan Research Centre, Li Ka Shing Knowledge Institute, [2]Critical Care Unit, St. Michael's Hospital, and [3]Department of Surgery, University of Toronto, Toronto, Ontario M5B 1W8, Canada
[4]Department of Immunology, Juntendo University School of Medicine, 113-8421 Tokyo, Japan

Epithelial–myofibroblast (MF) transition (EMyT) is a critical process in organ fibrosis, leading to α–smooth muscle actin (SMA) expression in the epithelium. The mechanism underlying the activation of this myogenic program is unknown. We have shown previously that both injury to intercellular contacts and transforming growth factor β (TGF-β) are indispensable for SMA expression (two-hit model) and that contact disruption induces nuclear translocation of myocardin-related transcription factor (MRTF). Because the SMA promoter harbors both MRTF-responsive CC(A/T)-rich GG element (CArG) boxes and TGF-β–responsive Smad-binding elements, we hypothesized that the myogenic program is mobilized by a synergy between MRTF and Smad3. In this study, we show that the synergy between injury and TGF-β exclusively requires CArG elements. Surprisingly, Smad3 inhibits MRTF-driven activation of the SMA promoter, and Smad3 silencing renders injury sufficient to induce SMA expression. Furthermore, Smad3 is degraded under two-hit conditions, thereby liberating the myogenic program. Thus, Smad3 is a critical timer/delayer of MF commitment in the epithelium, and EMyT can be dissected into Smad3-promoted (mesenchymal) and Smad3-inhibited (myogenic) phases.

Introduction

Epithelial–mesenchymal transition (EMT) is a major phenotypic change characterized by the loss of epithelial features, including apicobasal polarity and intercellular contacts, and by the gain of mesenchymal properties, such as head–tail polarity, increased contractility, and accumulation of extracellular matrix proteins (Lee et al., 2006; Xu et al., 2009). EMT plays a key physiological role in embryonic development and wound healing (Nakaya and Sheng, 2008) and has been identified as a central mechanism in various pathological processes including carcinogenesis (Klymkowsky and Savagner, 2009) and tissue fibrosis (Kalluri and Neilson, 2003). Importantly, EMT can progress further along a myogenic program, leading to the gen-

eration of myofibroblasts (MFs), which is hallmarked by the expression of α–smooth muscle actin (SMA). In this study, we will use the term epithelial–MF transition (EMyT) to indicate this myogenic form of EMT. Tissue accumulation of MFs and the level of SMA expression show strong correlation with the severity of fibrosis (Yang and Liu, 2001). Moreover, studies in genetically tagged mice indicated that a substantial portion of MFs originates from the epithelium in various models of lung and kidney fibrosis, suggesting an important role for EMyT in the disease process (Iwano et al., 2002; Kim et al., 2006). Despite the key significance of EMyT in the pathology of fibrosis, the molecular mechanisms that turn on and regulate the myogenic program (SMA expression) in the epithelium are incompletely understood.

The Rockefeller University Press $30.00
J. Cell Biol. Vol. 188 No. 3   383–399
www.jcb.org/cgi/doi/10.1083/jcb.200906155

JCB   **383**

THE JOURNAL OF CELL BIOLOGY

Increasing evidence indicates that EMT is a result of multiple, simultaneous inputs (Masszi et al., 2004; Kim et al., 2009a,b). Our previous experiments aimed at the identification of critical triggering factors showed that both an injury of intercellular contacts (e.g., their uncoupling by low calcium medium [LCM] or wounding) and TGF-β1 (TGF-β) are required to induce SMA expression in kidney epithelial cells (Masszi et al., 2004). Therefore, these data defined a two-hit model of EMyT, which is particularly suitable to dissect the key cellular events underlying MF differentiation. We then addressed the mechanism whereby contact injury impacts SMA expression and identified myocardin-related transcription factor (MRTF), a recently described myogenic transcriptional coactivator (Wang et al., 2002), as a key mediator of the process (Fan et al., 2007; Sebe et al., 2008). The proximal part of the SMA promoter contains two CC(A/T)-rich GG element (CArG) boxes, which are cis-elements targeted by serum response factor (SRF), a major regulator of cell growth and myogenic differentiation (Hautmann et al., 1999; Miano et al., 2007). The recent discovery of the myocardin family (myocardin, MRTF-A, and -B; Wang et al., 2001; Miralles et al., 2003) explained the old enigma of how SRF could fulfill these separate (growth promoting and myogenic) roles: binding of myocardin proteins confers muscle specificity to and enhances the activity of SRF. Moreover, MRTF, a major inducer of cytoskeletal genes, is itself regulated by the cytoskeleton. According to the current model, in quiescent cells, MRTF is bound to G-actin in the cytosol, but upon actin polymerization, it dissociates from G-actin and translocates to the nucleus (Posern and Treisman, 2006). We and others observed that disassembly of cell contacts in epithelial monolayers (e.g., by LCM) provokes robust nuclear translocation of MRTF in a Rho/Rho kinase– and Rac-dependent manner (Fan et al., 2007; Busche et al., 2008; Sebe et al., 2008). Importantly, MRTF is necessary for SMA expression during EMyT (Fan et al., 2007; Elberg et al., 2008). Nonetheless, injury-induced MRTF translocation alone is insufficient for SMA expression, as the process also requires TGF-β.

What is the mechanism whereby TGF-β synergizes with contact injury to induce myogenic reprogramming? We considered that signaling through receptor Smads (R-Smads), the direct targets of the activated TGF-β receptor kinase, might account for the synergy. This idea stems from the facts that (a) R-Smads mediate a variety of the fibrogenic effects of TGF-β (Xu et al., 2009), (b) the SMA promoter harbors Smad-binding elements (SBEs), which specifically bind Smad3 (Hu et al., 2003), and (c) Smad3 has been shown to directly bind to MRTF (Morita et al., 2007a). Cognizant of this scenario, we hypothesized that MRTF translocation and Smad3 signaling represent the contact injury– and TGF-β–dependent arms of the two-hit scheme. We considered that MRTF and Smad3 target their cognate cis-elements in the SMA promoter independently, but their effect might be more than additive. Alternatively, Smad3 might directly bind to MRTF, and the complex synergistically drives the promoter either through CArGs or SBEs. We also asked whether TGF-β signaling modifies the nucleocytoplasmic traffic of MRTF.

Surprisingly, we found that the CArG boxes are necessary and sufficient for the synergy between contact injury and TGF-β in SMA promoter activation, that Smad3 is a strong inhibitor of MRTF-driven SMA expression, and that Smad3 is degraded during EMyT. These results suggest a novel regulatory mechanism in myogenic reprogramming and define a Smad3-promoted and a Smad3-inhibited phase in EMyT.
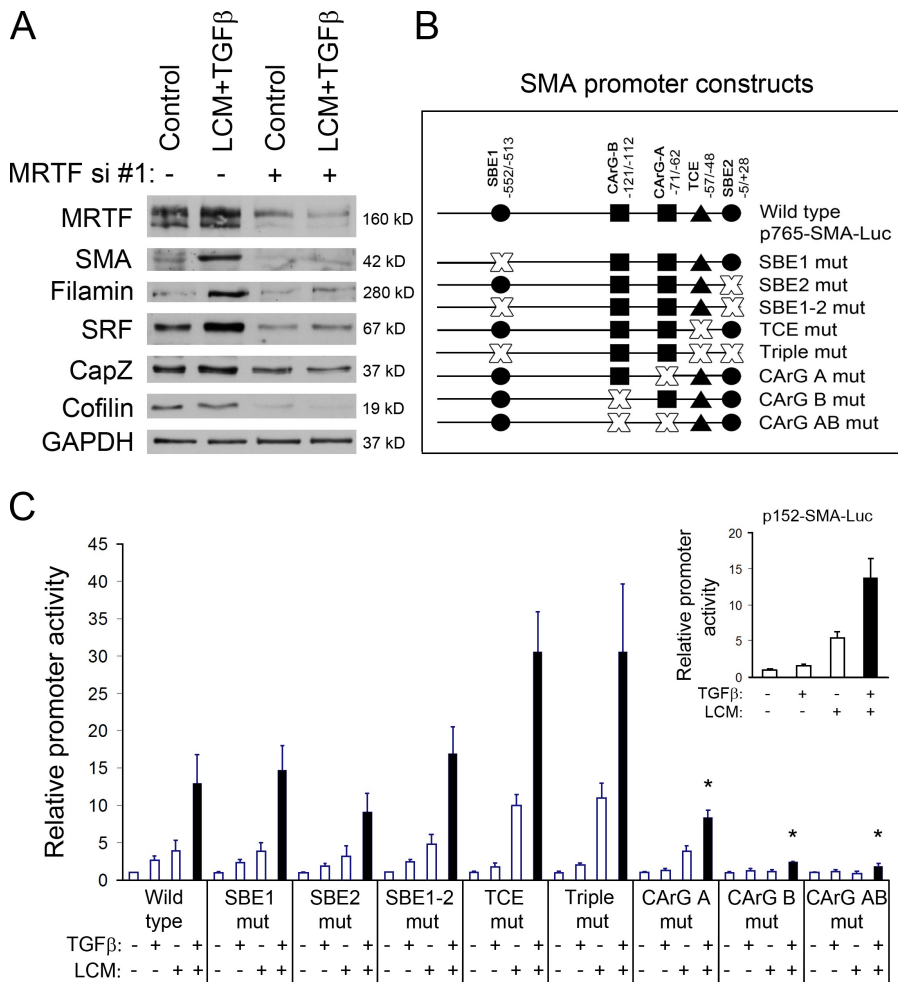
Results

MRTF plays a critical role in cytoskeletal reprogramming during EMyT

Our previous studies have established that both the disruption of intercellular contacts (by LCM) and exposure to TGF-β are required for EMyT in tubular cells. To determine the importance of MRTF in the expression of SMA in the context of this two-hit model, we transfected cells with control or MRTF-specific siRNA and treated them with LCM and TGF-β simultaneously for 48 h. We used two specific siRNA constructs, both of which provided a near-complete knockdown of MRTF (Fig. 1 A and Fig. S1). As expected (Masszi et al., 2004), in the presence of nonrelated (NR) siRNA, the combined treatment induced robust SMA expression. This response was abolished by the MRTF siRNAs. To assess whether the observed inhibitory effect is restricted to SMA expression or other CArG box–containing genes might also be affected, we checked the fate of some important representatives of the CArGome (Sun et al., 2006). Similar to SMA, filamin, SRF, the myosin heavy chain, and to a lesser extent, CapZ and α1-integrin, were up-regulated during EMyT, and these responses were strongly inhibited by the suppression of MRTF (Fig. 1 A and Fig. S1). The down-regulation of MRTF strongly reduced cofilin expression under both resting and stimulated conditions. These findings imply that MRTF is a master regulator of actin skeleton–related genes and thereby the cytoskeletal reprogramming during EMyT.

Stimulatory effect of both inputs converge on the CArG boxes

Next, we sought to identify the critical promoter elements responsible for the effect of LCM, TGF-β, and their synergy. The proximal portion of the SMA promoter contains several regulatory elements, including two CArG boxes, two SBEs, and a TGF-β control element (TCE; Fig. 1 B). As earlier studies performed by us and others have shown that LCM activates the Rho pathway (Fan et al., 2007; Busche et al., 2008), we hypothesized that LCM might primarily act via CArG boxes, whereas the effect of TGF-β might be predominantly mediated by SBEs and/or TCE. To characterize the importance of these elements, we generated a set of luciferase reporter constructs with various mutations of the SMA promoter (Fig. 1 B). The cells were transfected with wild-type (WT) or mutant SMA promoter plasmids along with the internal control plasmid, pRL-TK, and treated with TGF-β and/or LCM for 24 h (Fig. 1 C). In agreement with our previous results (Masszi et al., 2004; Fan et al., 2007), both TGF-β and contact injury induced a modest

A

MRTF si #1:

	Control	LCM+TGFβ	Control	LCM+TGFβ	
	−	−	+	+	
MRTF					160 kD
SMA					42 kD
Filamin					280 kD
SRF					67 kD
CapZ					37 kD
Cofilin					19 kD
GAPDH					37 kD

B SMA promoter constructs

Wild type p765-SMA-Luc
SBE1 mut
SBE2 mut
SBE1-2 mut
TCE mut
Triple mut
CArG A mut
CArG B mut
CArG AB mut

C

Figure 1. **MRTF is a key transcription factor for CArG-dependent genes in EMyT.** (A) Confluent LLC-PK1 cells transfected with NR (−) or MRTF siRNA (+) for 24 h were serum deprived for 3 h and treated with normal medium (control) or the combination of LCM and 10 ng/ml TGF-β (LCM + TGF-β) for 48 h followed by Western blotting for the indicated proteins. (B) The applied SMA promoter luciferase constructs. (C) The CArG boxes are critical, whereas genuine TGF-β–responsive elements are dispensable for the effect of individual stimuli and their synergy on the SMA promoter. Near-confluent monolayers were transfected with the indicated SMA constructs and renilla luciferase pRL-TK plasmid for 24 h and either left untreated or exposed to LCM, TGF-β, or the combination of these (black columns) for another 24 h. (inset) Activation of the 152-bp SMA promoter that contains only the CArGs and TCE. The firefly/renilla ratio of the control was taken as 1. Error bars indicate mean ± SEM.

increase in the promoter activity (2.6- and 4-fold, respectively), whereas the combined treatment acted synergistically (13-fold). First, we investigated the role of the genuine TGF-β–responsive regions, namely the two SBE and TCE sites. Interestingly, inactivating mutations of these elements alone or in combination neither inhibited the effect of the individual treatments nor affected their synergy. Moreover, promoter constructs harboring mutation in the TCE exhibited significantly higher activation than the WT when the cells were challenged with LCM or the combined treatment. In contrast, inactivation of the CArG sites strongly reduced the effect of all treatments. Mutation of the CArG-A box had a strong although incomplete inhibitory effect, whereas the CArG-B and double mutants were rendered entirely unresponsive to LCM, TGF-β, or their combination (Fig. 1 C). A short, 152-bp promoter segment, which contains the two intact CArG boxes but lacks SBE1 and the E boxes, remained sensitive to both stimuli (Fig. 1 C, inset). Together, these findings indicate that the CArG boxes are necessary and sufficient not only for the contact injury–induced (Rho/Rho kinase–mediated; Fan et al., 2007; Sebe et al., 2008) activation of the promoter but also for the TGF-β–triggered response and synergy between these stimuli. In contrast, all of the genuine TGF-β elements (SBE and TCE) are dispensable.

TGF-β prolongs the injury-induced nuclear accumulation of MRTF

Having seen that the effect of the two hits converges on CArG boxes, we wished to determine how these stimuli impact the nucleocytoplasmic transport of MRTF. We asked whether their synergy might be explained by their concerted effect on MRTF localization. To address this, we used both immunofluorescence microscopy (Fig. 2, A and B) and Western blotting of nuclear extracts (Fig. 2, C and D). The two approaches gave similar results: in untreated cells within intact, confluent monolayers, MRTF was cytosolic. LCM, when applied alone, induced rapid (30 min) and robust nuclear translocation of MRTF (Fig. 2). However, this response was transient, as at 2 h, there was a major reduction in the number of cells with nuclear MRTF (Fig. 2, A and B) and in the overall nuclear MRTF content (Fig. 2, C and D). Thereafter, MRTF remained at this slightly suprabasal level. TGF-β alone did not induce any translocation of MRTF in the first 2 h, and even after 6 h caused only a moderate translocation in a small fraction (∼10%) of the cells. This is in agreement with our pervious data showing that TGF-β in itself is unable to induce SMA expression in confluent monolayers (Fan et al., 2007). Importantly, the inability of TGF-β to elicit MRTF translocation was not caused by general unresponsiveness: TGF-β provoked strong nuclear translocation and phosphorylation of Smad3 (Fig. 2 E). Furthermore, when TGF-β was added together with LCM, both the number

Figure 2. **TGF-β augments and prolongs the injury-induced nuclear accumulation of MRTF.** (A) Confluent monolayers were exposed for various times to the indicated stimuli, stained for MRTF, and visualized by immunofluorescence microscopy. Bar, 30 μm. (B) Images were quantified as a percentage of cells with clear nuclear accumulation of MRTF. (C) Nuclear extracts were prepared from cells treated as shown. Nuclear MRTF was visualized by Western blotting from extracts containing equal (5 μg) protein. Equal loading was verified by histones (shown for the LCM condition). WCL, whole cell lysate. (D) Densitometric quantification of C. Values are expressed relative to the density of the MRTF signal in 5 μg WCL (100%) loaded on the same membrane (n ≥ 3). (E) TGF-β induces early and robust nuclear translocation and phosphorylation of Smad3 in confluent LLC-PK1 cells. Nuclear extracts were prepared from cells treated as shown and probed with total and phospho-Smad3 antibodies. Error bars indicate mean ± SEM.
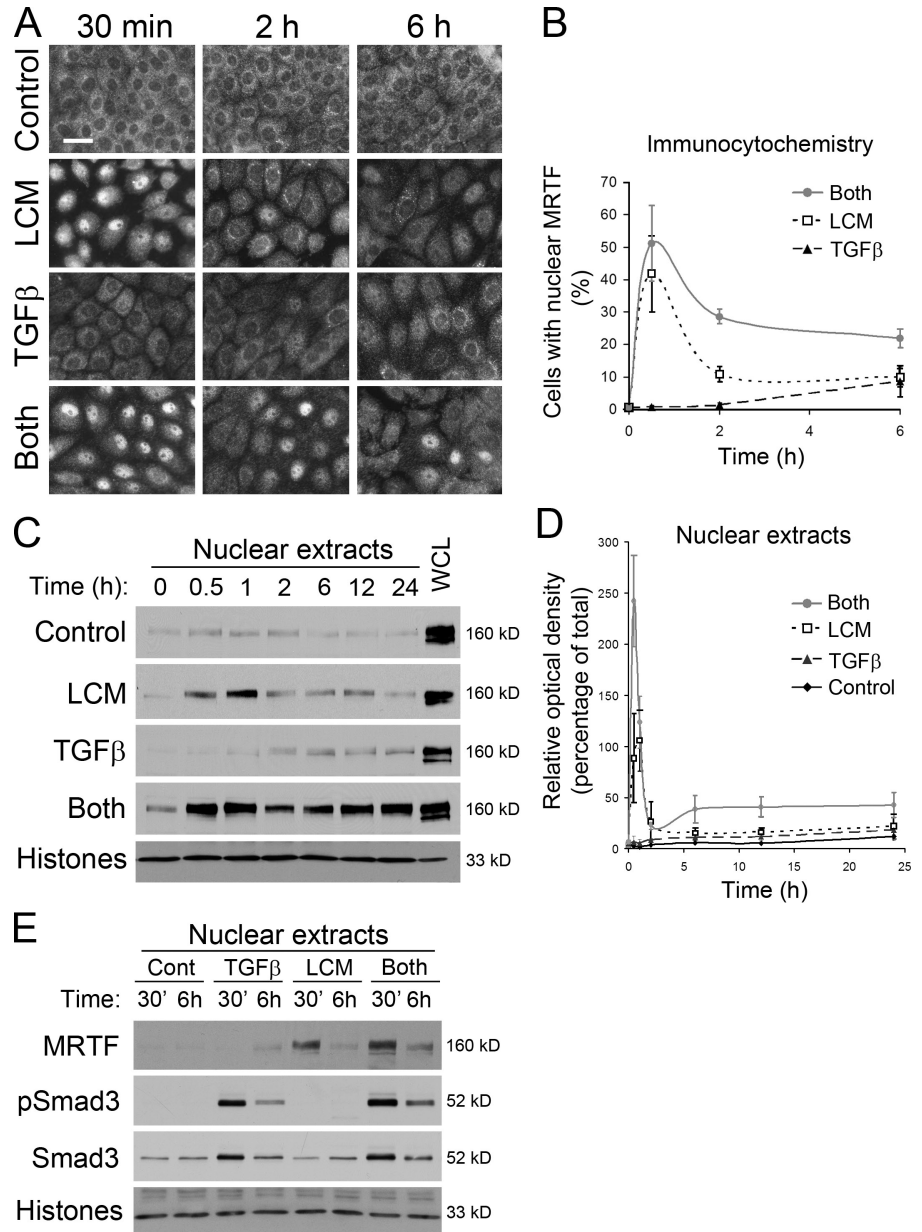
of cells with strong nuclear MRTF translocation and the overall nuclear MRTF content was higher than after LCM stimulation at the peak, and importantly, it remained significantly above the LCM-induced level for the investigated period (24 h). It is noteworthy that when combined with LCM, TGF-β markedly promoted nuclear MRTF accumulation even at times when alone it had no effect. These findings show that although TGF-β is a very weak stimulus to induce MRTF translocation in the intact epithelium, it augments and prolongs the nuclear accumulation of MRTF provoked by contact injury. This effect likely contributes to the synergy between the combined stimuli and the ensuing EMyT.

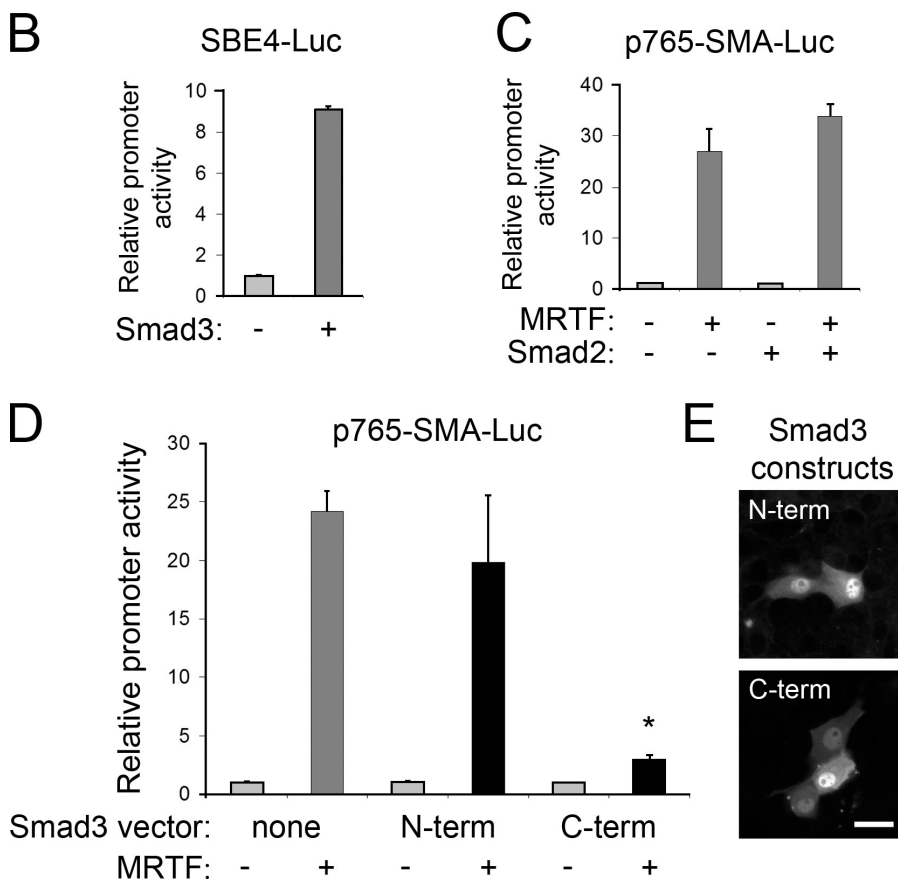## Smad3 is a strong inhibitor of the SMA-inducing effect of MRTF: a surprising finding

Smad3, one of the central mediators of TGF-β signaling, has been shown to directly bind to MRTF (Morita et al., 2007a).

Given the facts that (a) LCM and TGF-β induce the nuclear translocation of MRTF and Smad3, respectively, (b) these factors can interact, and (c) the SMA-inducing effects are mediated via CArGs, we hypothesized that a Smad3–MRTF complex might exert an augmented effect on CArG cis-elements. Indeed, similar potentiation by Smads through non-SBE sites has been described previously in other promoters (Qiu et al., 2003). To test whether Smad3 can indeed facilitate the transcriptional effect of MRTF, cells were cotransfected with the 765-bp (WT) SMA-Luc/renilla reporter system along with constructs encoding Flag-tagged MRTF, Myc-tagged Smad3, or both (Fig. 3 A). As expected, MRTF robustly induced the SMA promoter. Smad3 itself did not affect SMA promoter activity (<1.4-fold increase), whereas it strongly stimulated SBE4-Luc, a Smad3-responsive promoter construct (Fig. 3 B). To our surprise, when coexpressed with MRTF, Smad3 potently inhibited the MRTF-induced activation of the SMA promoter

A

Relative promoter activity (0–100)

p765-SMA-Luc | Triple mut | p152-SMA-Luc
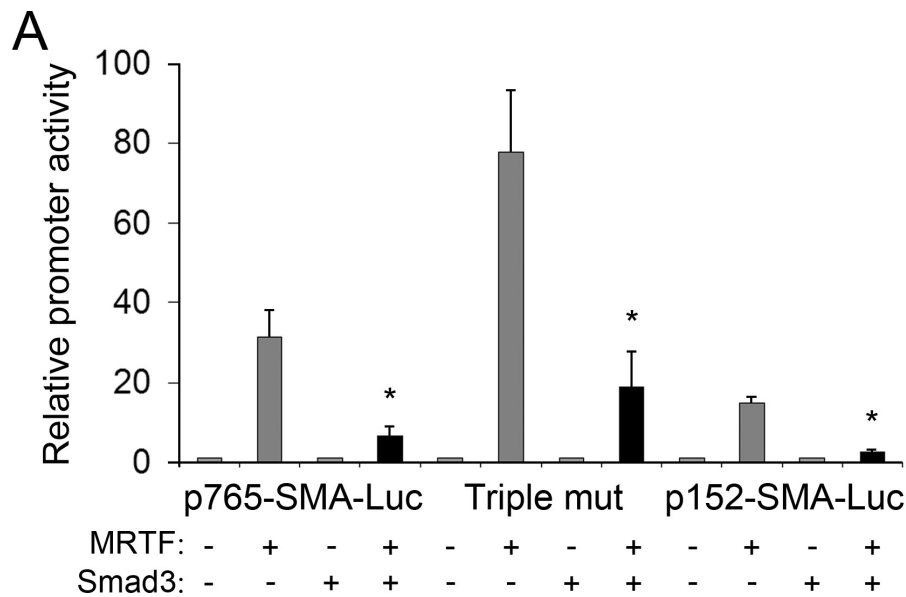
| MRTF: | - | + | - | + | - | + | - | + | - | + | - | + |
| Smad3: | - | - | + | + | - | - | + | + | - | - | + | + |

Figure 3. **Smad3 strongly inhibits the MRTF-induced stimulation of the SMA promoter, and this effect requires the CArG box and the Smad3 C terminus.** (A) Cells were transfected with WT or mutant SMA-Luc and pRL-TK constructs along with empty vector, MRTF, and/or Smad3 for 48 h. (B) Smad3 expression potently stimulates the SBE4-Luc reporter. Cells were cotransfected with empty vector or Smad3 and the SBE4-Luc/pRL-TK system. (C) Cells were cotransfected with SMA-Luc and with empty vector, MRTF, and/or Smad2 for 48 h. (D) Cells were cotransfected with empty vector (none), N-terminal (N-term; 1–210 aa) or C-terminal (C-term; 211–425 aa) Smad3 construct, the SMA-Luc/pRL-TK system, and MRTF or empty vector as indicated. (E) Similar localization of N- and C-terminal Smad3 constructs as visualized by immunostaining for their Myc tag. Bar, 20 μm. Error bars indicate mean ± SEM.

B
SBE4-Luc

| Smad3: | - | + |

C
p765-SMA-Luc

| MRTF: | - | + | - | + |
| Smad2: | - | - | + | + |

D
p765-SMA-Luc

| Smad3 vector: | none | | N-term | | C-term | |
| MRTF: | - | + | - | + | - | + |

E
Smad3 constructs

N-term

C-term

(Fig. 3 A). This effect was specific for Smad3, as overexpression of Smad2 did not inhibit the SMA promoter (Fig. 3 C). To address whether Smad3 might inhibit MRTF by affecting any of the two SBEs or the TCE box (i.e., in a CArG-independent manner), we used our triple-SMA promoter mutant in which these elements are inactivated. Smad3 efficiently suppressed the MRTF-induced response of this mutant as well. Furthermore, the same inhibitory effect was observed on the 152-bp promoter, indicating that no additional upstream elements (e.g.,

E boxes) are required for the inhibition (Fig. 3 A). These findings imply that Smad3 interferes with the stimulatory effect of MRTF mediated via the CArGs.

Morita et al. (2007a) have reported that MRTF binds to the C-terminal but not the N-terminal half of Smad3. To assess whether the inhibitory effect of Smad3 might depend on the same region, we tested the effects of N- and a C-terminal Smad3 constructs (Fig. 3 D). The N-terminal half failed to inhibit the effect of MRTF, whereas the C-terminal half recapitulated the

Figure 4. **Myogenic (two hit) conditions induce dramatic loss of Smad3 and mitigate the MRTF–Smad3 interaction.** (A) Cells were treated according to the two-hit scheme for the indicated times, and Smad3 expression was assessed by Western blotting. (B) Smad3 degradation is selective. The various stimuli were applied for 24 h. (C–E) Smad3 is regulated at both mRNA and posttranscriptional levels. (C) Smad3 mRNA content was determined by qPCR after 24 h treatment and normalized to GAPDH content and the control sample. (D) Cells transfected with Flag-Smad3 vector were treated for 24 h as indicated. Flag-Smad3 levels were measured by probing for the tag. (E) Cells were preincubated with 5 µg/ml cycloheximide and treated as indicated for 12 h. Overall protein loss as a result of the inhibition of de novo synthesis was compensated by loading equal amount of protein. (F) MRTF–Smad3 association in the two-hit model. Cells were treated as indicated for 1 or 24 h followed by immunoprecipitation with anti-MRTF antibody. Precipitates were probed for MRTF and the coprecipitating Smad3. (top) Densitometric quantification of the cosedimenting Smad3 normalized to the control. Note that long-term combined treatment eliminates the LCM-triggered increase in the association of Smad3 and MRTF. Error bars indicate mean ± SEM.
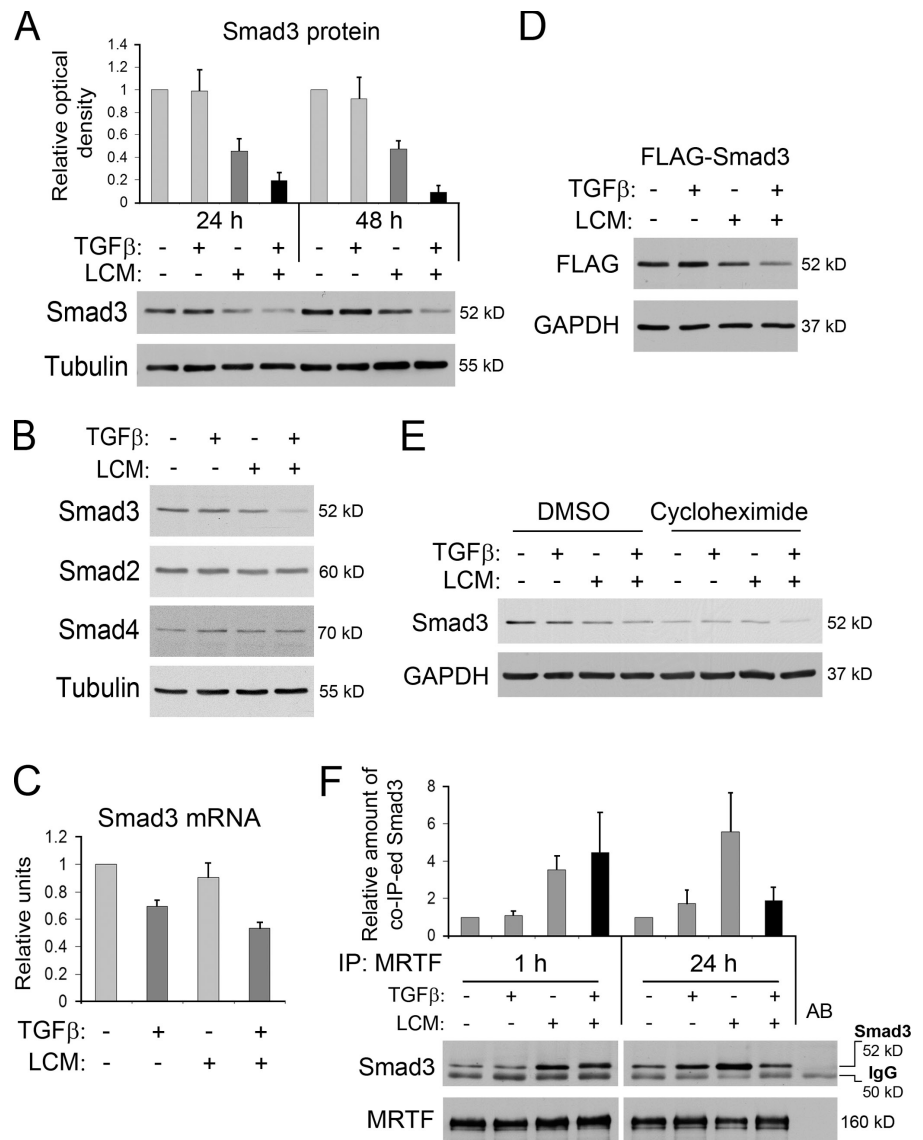
effect of the full-length protein. This differential effect was not the result of distinct nuclear localization of these Smad3 proteins because immunostaining against their Myc epitope revealed that they were similarly expressed and both localized in the cytoplasm and the nucleus with nuclear predominance (Fig. 3 E).

Next, we verified that Smad3 overexpression does not inhibit and in fact facilitates the nuclear translocation/retention of MRTF (Fig. S2). Thus, Smad3 may contribute to the prolonged nuclear retention of MRTF seen upon TGF-β stimulation (Fig. 2, A–D), but it strongly inhibits the promoter-inducing effect of MRTF.

Smad3 expression is diminished under myogenic (two hit) conditions

Our experiments suggested that Smad3, a central mediator of TGF-β signaling, might be a negative regulator of the SMA promoter. However, we have also shown that TGF-β is necessary for SMA expression. To address this apparent discrepancy, we investigated the fate of Smad3 during EMyT by measuring the

level of Smad3 protein expression under the two-hit conditions (Fig. 4 A). Intriguingly, LCM itself induced a 50% reduction in Smad3. TGF-β alone had marginal effect after 24 h and caused a slight decrease after 48 h. When LCM and TGF-β were combined, Smad3 expression dropped dramatically, exhibiting 90% reduction after 48 h. This effect was selective for Smad3, as the level of Smad2 and Smad4 remained unaltered (Fig. 4 B).

To address the mechanisms responsible for decreased Smad3 protein, we first measured the effects of the two-hit scheme on Smad3 mRNA. TGF-β significantly reduced Smad3 mRNA, whereas LCM had only marginal effect. The combined treatment led to a 50% reduction after 24 h (Fig. 4 C). Because the overall loss in Smad3 protein exceeded this level, we also investigated the potential contribution of enhanced protein degradation using two approaches. We expressed Flag-Smad3, which is driven by an artificial (cytomegalovirus) promoter or treated the cells with the protein synthesis inhibitor cycloheximide and then tested whether the various stimuli could (further) reduce Smad3 levels. LCM and the combined treatment (but not TGF-β) induced strong reduction in Flag-Smad3 protein

(Fig. 4 D). Moreover, the combined treatment facilitated the loss of endogenous Smad3 even in the presence of cycloheximide (Fig. 4 E). These results show that myogenic stimuli induce dramatic loss in Smad3 protein through both transcriptional and posttranscriptional mechanisms, and this process precedes the expression of SMA.

Interaction between Smad3 and MRTF in the two-hit model

Our findings suggest that TGF-β–enhanced Smad3 degradation might be an important contributor to MF transition presumably through the disinhibition of MRTF. To address this idea, we first examined whether the association between MRTF and Smad3 changes in the context of the two-hit model (Fig. 4 F). Under resting conditions, immunoprecipitates of endogenous MRTF contained some endogenous Smad3. Short-term (1 h) stimulation with LCM or the combination, but not TGF-β alone, increased the association between the two proteins. Importantly, in cells treated with LCM alone, the association remained high or increased even further after 24 h. In contrast, in the presence of LCM and TGF-β, the amount of coprecipitating Smad3 dropped back to the level found in unstimulated cells. The most plausible interpretation of this finding is that because of Smad3 degradation, less Smad3 was available for binding. Collectively, long-term combined stimulation leads to increased MRTF level in the nucleus without increased MRTF–Smad3 association.

Elimination of Smad3 enhances the activity of the SMA promoter

So far, we showed that Smad3 overexpression inhibits the effect of MRTF and that Smad3 degrades in the two-hit model. In the following experiments, we sought to examine whether decreasing Smad3 levels indeed play a role in the genetic reprogramming during EMyT. We first determined whether the level of Smad3 degradation, as observed in the two-hit model, correlates with the ensuing SMA promoter activation. To this end, we treated the cells according to the two-hit scheme (LCM, TGF-β, or both) and prepared lysates at various times (2, 6, 12, 24, and 48 h) after stimulation. Smad3 expression was determined in each sample by Western blotting as in Fig. 4 A. In parallel experiments, cells had been transfected with the 765-bp SMA-Luc reporter and treated as for the Western blots, after which the activity of the SMA promoter was measured. Having obtained these two datasets, we plotted the activation of the SMA promoter against the level of the corresponding Smad3 expression (Fig. 5 A). The resulting function was best fitted with a hyperbola (see also the linearized form; $r^2 = 0.93$), signifying a reciprocal relationship between the level of Smad3 and the corresponding promoter response.

Next, we tested whether reduction in Smad3 is indeed the causal factor that permits increased activation of the endogenous SMA promoter. Cells were treated with Smad3 siRNA (causing 90% reduction in Smad3 expression; Fig. 5 B) and challenged with LCM for 3 or 6 h. Subsequently, SMA mRNA content was determined by quantitative PCR (qPCR; Fig. 5 C). We used LCM as stimulus, as it only partially reduces Smad3,

while it provides sufficient MRTF translocation. In control cells, LCM induced a 10-fold increase in SMA mRNA after 6 h. Down-regulation of Smad3 in the absence of stimulus caused a similar increase. Intriguingly, after Smad3 depletion, LCM provoked a dramatic rise (2,500-fold over baseline) in SMA mRNA, amounting to a 250-fold stimulation compared with the effect of Smad3 elimination alone.

To test whether the reduction in Smad3 indeed impacted the interaction between MRTF and the endogenous SMA promoter, we used a chromatin immunoprecipitation (ChIP) assay (Fig. 5 D). Cells were transfected with control or Smad3 siRNA and exposed to normal medium or LCM. MRTF was immunoprecipitated, and the precipitates were analyzed with a PCR probe against the proximal CArG box of the SMA promoter (Elberg et al., 2008). MRTF immunoprecipitates from control cells captured some SMA CArG-A element, the level of which increased upon LCM treatment. The coprecipitated CArG-A signal did not detectably increase by Smad3 elimination alone; however, the effect of LCM was much stronger in the Smad3-depleted cells (Fig. 5 D). Collectively, these findings indicate that stimulus-induced or siRNA-provoked reduction in Smad3 expression facilitates the association between MRTF and the CArG-A box of the endogenous SMA promoter, stimulates the promoter, and increases SMA mRNA.

Suppression of Smad3 potentiates the expression of SMA and other CArGome proteins

To investigate whether a reduction in Smad3 indeed translates into elevated SMA protein levels, we compared the expression of SMA in the presence of control or Smad3 siRNA in cells treated according to the two-hit scheme (Fig. 6 A). Although in control cells SMA was just becoming detectable after a 48-h exposure to these stimuli (Masszi et al., 2004), in the Smad3 knockdown group, robust SMA expression occurred (Fig. 6 A). Moreover, in Smad3 down-regulated cells, LCM in itself was sufficient to provoke SMA protein expression. Because LCM alone never causes SMA expression in control cells, this striking observation implies that the absence of Smad3 makes TGF-β unnecessary for SMA expression and renders contact injury, as a single hit, sufficient for MF generation. Identical results were obtained when another Smad3-specific siRNA was used (unpublished data). To test whether SMA expression in Smad3-depleted cells still remained dependent on MRTF, cells were cotransfected with MRTF and Smad3 siRNAs. The absence of MRTF prevented SMA expression in the Smad3 knockdown cells as well, when LCM or LCM + TGF-β were used as stimuli (Fig. 6 A). This verifies that the absence of Smad3 did not divert the myogenic program to an alternate pathway; instead, it increased the efficiency of the MRTF-dependent mechanism. Importantly, the robust potentiation of SMA expression by the loss of Smad3 was also observed in BEAS-2B lung epithelial cells and human gingival fibroblasts (Fig. 6 B), implying that this is a general phenomenon. Smad2 silencing had no such effect (Fig. 6 C). The loss of Smad3 also facilitated the expression of cofilin and SRF, suggesting that Smad3 can also inhibit the

Figure 5. **Reduced Smad3 expression robustly facilitates SMA promoter activity, SMA mRNA expression, and the interaction between MRTF and the endogenous SMA promoter.** (A) Relative Smad3 levels were determined by Western blotting after LCM or combined treatment at various times (0–48 h) and plotted against the corresponding SMA promoter activity measured in parallel after the same treatments. Each point represents the means of three determinations. Power function fit resulted in a hyperbola. (inset) Linearization of the relationship using the reciprocal of the promoter activity. (B) Efficiency of Smad3 silencing. (C) Smad3 silencing strongly potentiates LCM-induced mRNA expression. Cells were treated with NR or Smad3 siRNA and left untreated or exposed to LCM for 3 or 6 h and processed for RNA extraction. SMA mRNA was determined by qPCR and normalized to GAPDH. Data are expressed as fold change (logarithmic scale) compared with control. (D) Smad3 silencing enhances MRTF binding to the SMA promoter. Cells were transfected as in B, exposed to normal medium or LCM for 1 h, and processed for ChIP assays using anti-MRTF antibody. (top) Antibody-associated SMA promoter signals were quantified by qPCR (shown as fold cycle threshold change). (middle) Amplicons shown on agarose gels after 30 PCR cycles from the input and the MRTF antibody precipitates. (bottom) Western blots verifying Smad3 down-regulation. Error bars indicate mean ± SEM.
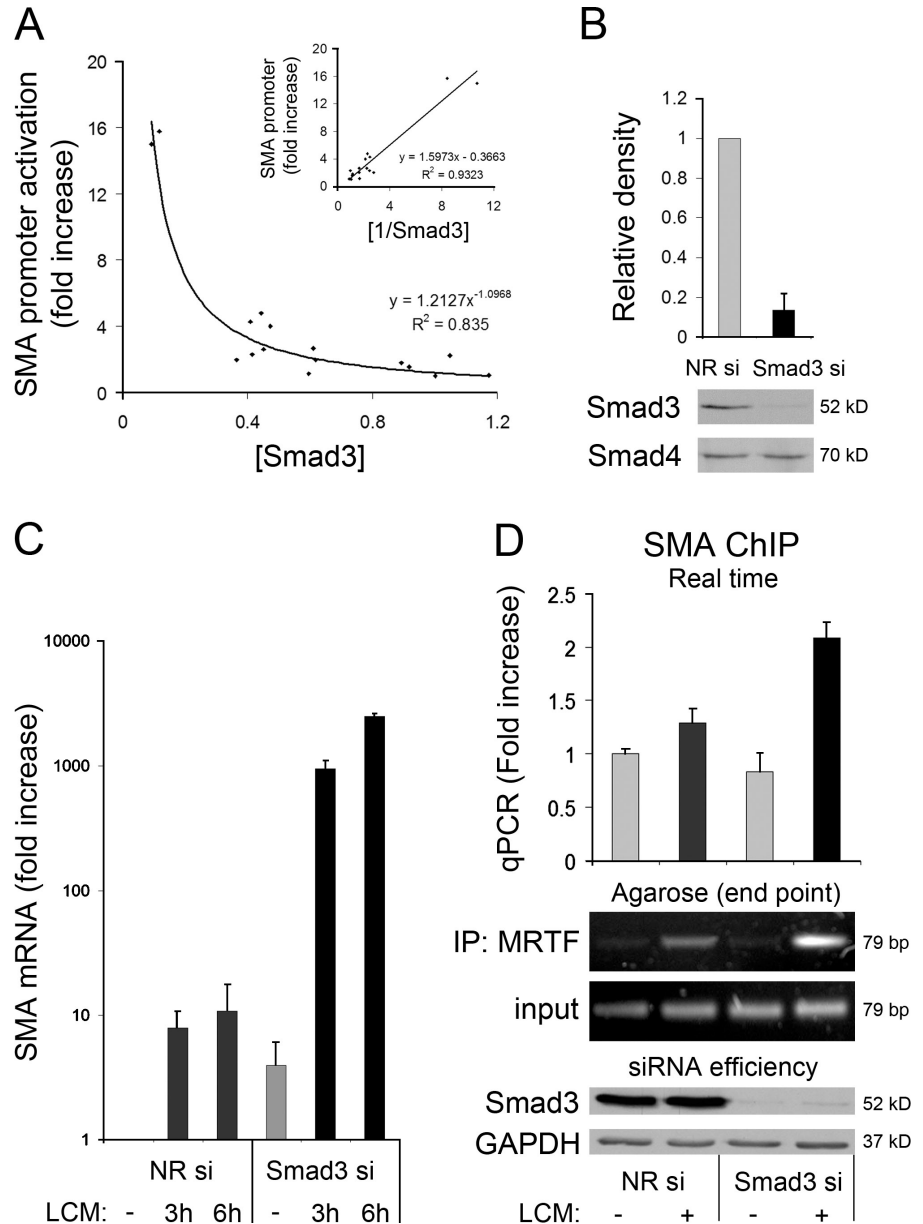
expression of other CArGome proteins (Fig. 6 D). Finally, E-cadherin down-regulation was less robust in Smad3-depleted cells (Fig. 6, A and E), a finding consistent with (but less pronounced than) that reported by Morita et al. (2007a) in MDCK cells. Together, these results indicate that elimination of Smad3 strongly stimulates EMyT, or conversely, Smad3 acts as a break or delayer of MF generation.

Smad3 interferes with the SRF–MRTF interaction

To gain insight into the molecular mechanism whereby Smad3 inhibits the function of MRTF, we asked whether it interferes with the MRTF–SRF interaction. To test this, we transfected cells with Myc-MRTF and HA-SRF and followed their association after silencing (Fig. 7 A) or overexpressing Smad3 (Fig. 7 B). The former condition strongly facilitated, whereas the latter markedly reduced the association of SRF with MRTF. To test whether

association between MRTF and Smad3 are indeed critical for the Smad3-induced inhibition, we deleted a 7-aa-long region (S279–P285) within the B1 box of MRTF-B (ΔB1p; Fig. 7 C). This section of the B1 box was selected because Morita et al., (2007a) have described that the B1 box is critical for Smad3 binding; however, it is also essential for the SRF–MRTF association, and therefore, ΔB1 is transcriptionally inactive (Zaromytidou et al., 2006). To overcome this problem, we eliminated only the proximal part of B1, which does not contain the LKYHQYI sequence, the critical core for SRF binding (Zaromytidou et al., 2006). Indeed, ΔB1p retained substantial SMA promoter–inducing activity (Fig. 7 D), whereas it exhibited a dramatically reduced binding to Smad3 (Fig. 7 C). Importantly, ΔB1p was much less sensitive to the inhibitory action of Smad3 than the WT (27 vs. 78% inhibition; Fig. 7 D). These findings imply that binding of Smad3 to MRTF is a critical mechanism in the Smad3-mediated inhibition of the SMA promoter (see Discussion).
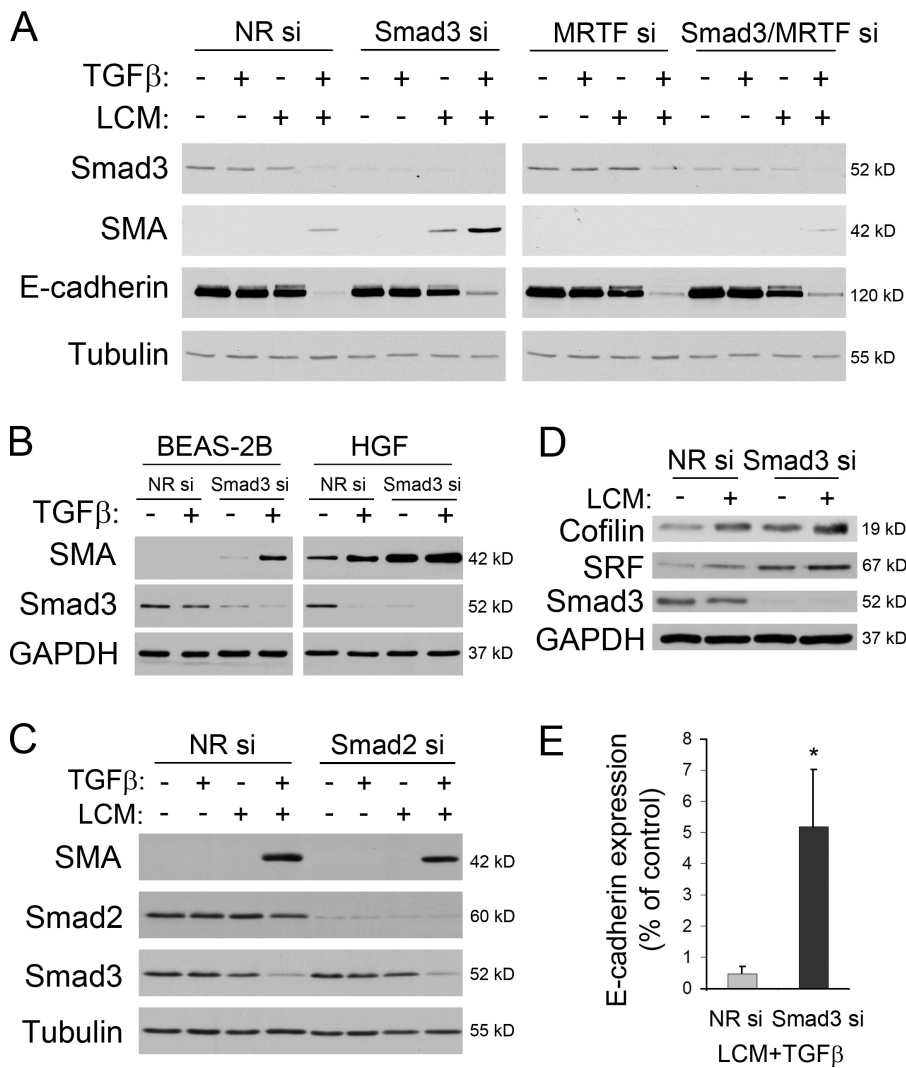
Figure 6. **The one-hit scenario. Smad3 silencing renders injury sufficient to induce MRTF-dependent SMA expression and potentiates the expression of other CArG-dependent genes.** (A) Confluent monolayers were exposed to NR, Smad3, MRTF, or Smad3 + MRTF siRNAs for 24 h followed by 48 h treatment according to the two-hit scheme. Cell lysates were prepared and probed by Western blotting for the indicated proteins. (B) Human lung epithelial cells (BEAS-2B) and gingival primary fibroblasts (HGF) were transfected with NR or Smad3 siRNA and 24 h later treated with TGF-β for 48 h. Whole cell lysates were probed for the indicated proteins. (C) Smad2 silencing does not facilitate SMA expression. Cells were transfected with siRNA against Smad2 and treated as in A for 2 d. Whole cell lysates were probed. (D) Cells were transfected as indicated and left untreated or exposed to LCM and processed for Western blotting using antibodies against cofilin and SRF. (E) E-cadherin loss is less complete in Smad3 siRNA cells. E-cadherin blots were analyzed by densitometry and normalized to control values. Error bars indicate mean ± SEM.

Opposite roles of Smad3 in the induction of mesenchymal and muscle characteristics

Although our findings indicate a potent inhibitory role for Smad3 in the process of EMyT, Smad3 has been also implicated as a strong profibrotic transcription factor that contributes to EMT. To explain this apparent discrepancy, we considered that Smad3 might play distinct roles in the first (mesenchymal) and second (myogenic) phase of the process. To address this, we followed the impact of Smad3 knockdown on the transcription of PAI-1 (plasminogen activator inhibitor-1), a TGF-β–responsive, profibrogenic gene, and SMA, the hallmark of MFs. Smad3 silencing induced opposite responses to TGF-β in these genes (Fig. 8 A). Both the basal level of the PAI-1 mRNA and its TGF-β–induced rise were strongly suppressed. Accordingly, Smad3 siRNA reduced PAI-1 protein expression induced by TGF-β or the combined treatment (Fig. 8 B). Similarly, the absence of Smad3 prevented the LCM/TGF-β–induced up-regulation of connective tissue growth factor (CTGF), another mediator of EMT (Fig. 8 B). In contrast, Smad3 silencing resulted in a significant increase in SMA mRNA in nonstimulated cells, which was further augmented by TGF-β (Fig. 8 A).

TGF-β failed to induce SMA mRNA in control cells, whereas it had a substantial effect in the absence of Smad3. These data indicate that Smad3 is essential for the expression of key proteins of mesenchymal transition, whereas it inhibits the myogenic reprogramming.

Because many cytoskeletal genes are regulated by CArG boxes, we investigated whether Smad3 down-regulation might induce F-actin reorganization toward an MF-like phenotype. After Smad3 silencing, many epithelial cells acquired elongated shape, lost their peripheral actin ring, and formed strong central stress fibers (Fig. 8 C). In addition, these cells tended to migrate away from the edges of clusters and did not form typical islands with rounded boundaries. Control epithelial cells at the periphery of the islands contained few and small focal adhesions, which were parallel to the cell edges. In contrast, Smad3-depleted cells had many large and more mature focal adhesions (as detected by total and phospho-FAK, paxillin, and α-actinin staining) that were perpendicular to the irregular cell edges. Collectively, the loss of Smad3 facilitates MF-like remodeling of the actin cytoskeleton, but these cells lack important features of the mesenchymal transition such as the up-regulation of PAI-1 and CTGF.

Figure 7. **Smad3 interferes with MRTF–SRF interaction.** (A) Cells were transfected with Myc-MRTF and HA-SRF along with NR or Smad3 siRNA. Association of MRTF and SRF was analyzed by coimmunoprecipitation. Smad3 silencing was detected from whole cell lysates (WCL). Controls for the immunoprecipitation were reaction without antibody (No AB) or Myc transfection (No Tx). (right) Densitometric analysis of three experiments is shown. (B) Myc-MRTF and HA-SRF were cotransfected with empty vector or Smad3. MRTF was immunoprecipitated with anti-Myc antibody as in A from control or LCM-treated (1 h) cells. (C) A 7-aa sequence in the B1 region is critical for Smad3 binding. The SRF-binding core is underlined. The predicted Smad3-binding site (S279-P285) is shown in italic. (top) This latter region was deleted to generate ΔB1p mutant. Coimmunoprecipitation shows decreased association of Smad3 to ΔB1p compared with WT. (D) ΔB1p mutant shows reduced sensitivity to inhibition by Smad3. Cells were transfected with SMA-Luc, ΔB1p, or WT MRTF along with empty vector or Smad3. Luciferase assay was performed 48 h later. Results are normalized to the control (top; fold increase over control) or expressed as a percentage of the maximal effect of the given MRTF construct (bottom). *, $P < 0.05$. Error bars indicate mean ± SEM.
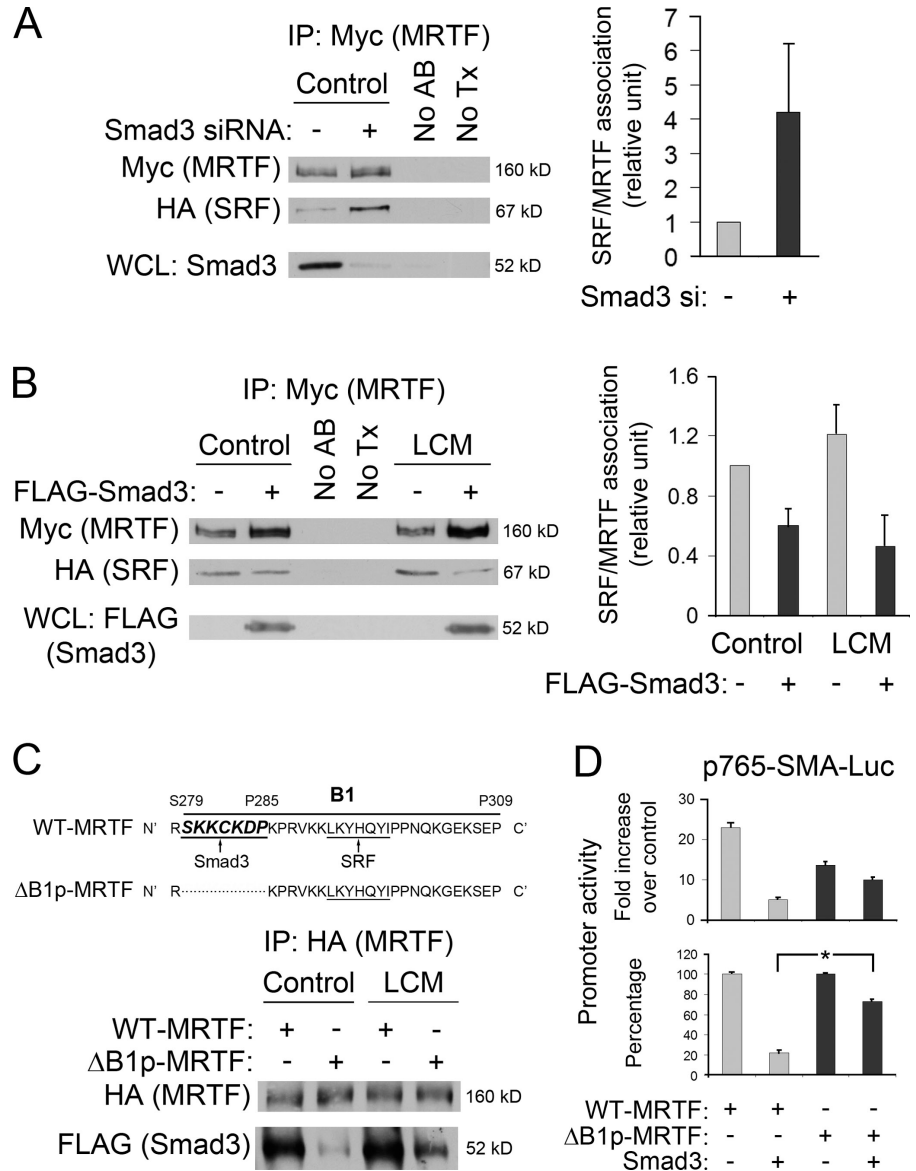
Discussion

MRTF has emerged as an indispensible mediator of actin skeleton remodeling and myogenic reprogramming during EMyT (Fan et al., 2007; Morita et al., 2007a,b; Elberg et al., 2008). Indeed, our current studies indicate that in addition to SMA, MRTF is necessary for the increased or sustained expression of a whole array of cytoskeletal proteins, the genes of which contain CArG boxes in their promoter (Fig. 1). Therefore, it has become a central question how MRTF signaling, a primarily Rho- and Rac-controlled process (Hill et al., 1995; Miralles et al., 2003; Fan et al., 2007; Busche et al., 2008; Sebe et al., 2008), collaborates with (other) TGF-β–induced pathways, which are also indispensible for EMyT. Our experiments have provided two significant and rather surprising insights into this mechanism: (1) detailed mutational analysis of the SMA promoter revealed that not only the contact injury–induced MRTF translocation but also the TGF-β–induced pathways target the MRTF–SRF-dependent CArG boxes (Fig. 1). Thus, all effects converge on these elements, which are necessary and sufficient for the synergy between these inputs. Indeed, inactivation of SBEs had no significant effect, whereas disruption of TCE, the binding site for Krüppel-like factors, facilitated the activation of the promoter, suggesting that these transcriptional regulators may have an inhibitory effect (Liu et al., 2005). (2) One of the critical mechanisms through which TGF-β facilitates MRTF signaling and SMA expression is that it reduces the expression of Smad3, i.e., a major mediator of its own signaling. Importantly, our results show that Smad3 is a strong inhibitor of the SMA-inducing effect of MRTF (Figs. 3 and 5–8) because (a) an inverse relationship exists between endogenous Smad3 expression and the activation of the SMA promoter, (b) overexpression of Smad3 abrogates the SMA promoter–stimulating effect of MRTF, and (c) down-regulation of Smad3 renders contact injury (as a single hit) sufficient to induce SMA expression, increases SMA mRNA, and facilitates the binding of MRTF to the endogenous SMA promoter. In addition, TGF-β prolongs the nuclear accumulation of MRTF (Fig. 2). This may be
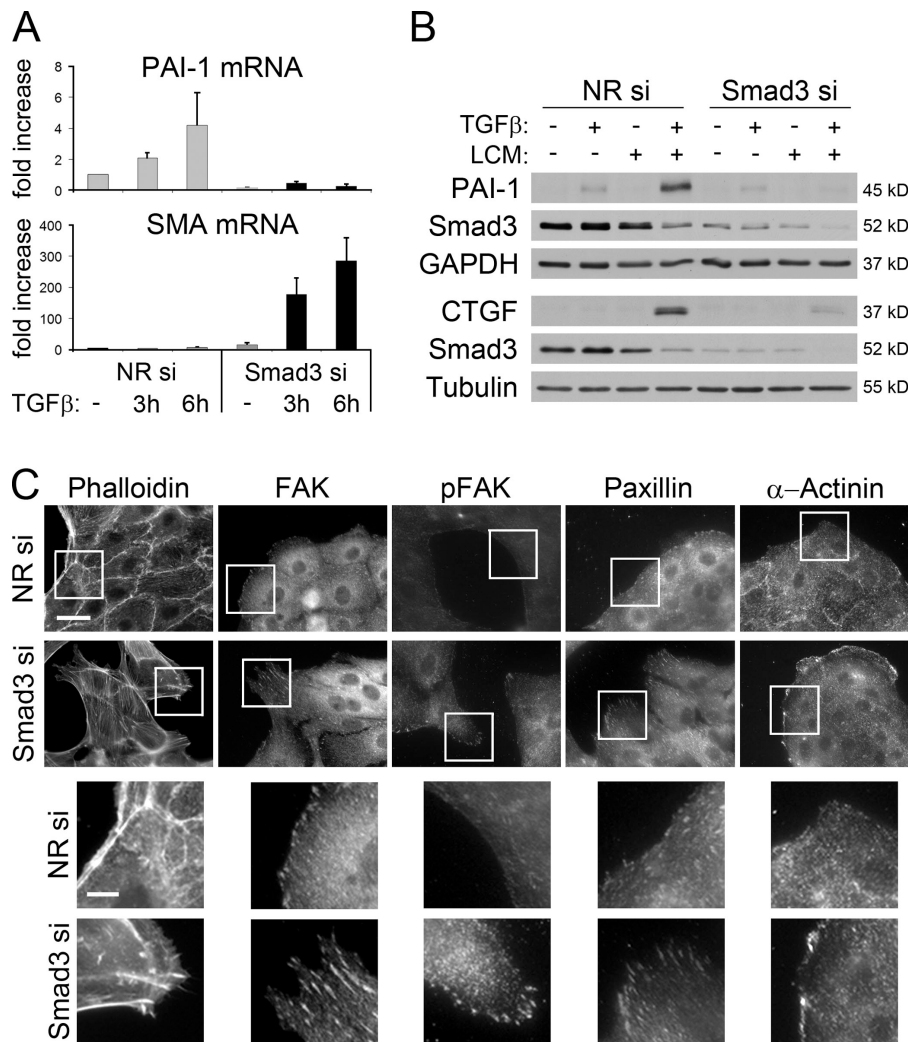
Figure 8. **Smad3 silencing has opposite effects on the expression of mesenchymal marker PAI-1 and on MF characteristics (SMA and cytoskeleton remodeling).** (A) PAI-1 and SMA mRNA was measured by qPCR in control and Smad3-depleted cells (Fig. 5 C) and treated with vehicle or TGF-β for 3 or 6 h. Note that although Smad3 depletion strongly stimulates TGF-β–induced SMA mRNA expression, the effect is still much less (∼0.125) compared with LCM (Fig. 5 C), in accordance with the fact that TGF-β alone (as opposed to LCM) does not induce SMA expression even in Smad3-depleted cells. (B) Expression of PAI-1 and CTGF protein under two-hit condition in Smad3-containing and -depleted cells. Cells were transfected with NR or Smad3 siRNA for 24 h, treated for an additional 48 h as indicated, and processed for Western blotting. (C) Smad3 depletion induces reorganization of the cytoskeleton. Cells were transfected with NR (top) or Smad3 siRNA (bottom) for 48 h, and F-actin and focal adhesions were visualized by rhodamine phalloidin or staining for FAK, phosphorylated FAK (pFAK), paxillin, or actinin. Loss of Smad3 induces the formation of central stress fibers and thick, elongated focal adhesions in cells located at the edges of islands. (bottom) Higher magnification images are shown of boxed areas. Bars: (top) 30 µm; (bottom) 10 µm. Error bars indicate mean ± SEM.

caused by additional actin polymerization as well as increased Smad3-dependent MRTF retention (Fig. S2). This may predispose the cells to enhanced MRTF-mediated transactivation once the decreasing levels of Smad3 liberate MRTF from its inhibited state. As our observations are somewhat unexpected, it is important to integrate them into the current knowledge about the mechanisms underlying EMT and EMyT.

Regarding the central role of CArGs, our findings are in agreement with a recent study (Elberg et al., 2008), which found that both CArGs were necessary for TGF-β–induced SMA promoter activation in human renal tubular cells. However, an unusual feature of that system, as opposed to other tubular (LLC-PK1 [Fan et al., 2007] and MDCK [Morita et al., 2007a]) cells is that MRTF was constitutively nuclear, even in unstimulated cells. Nonetheless, TGF-β remained necessary to induce SMA promoter activation and protein expression, implying that an additional (yet unidentified) TGF-β–dependent mechanism is still necessary even in the presence of nuclear MRTF. We propose that the TGF-β–induced reduction in Smad3 and the consequent disinhibition of MRTF may be such an input for MRTF activation. Our findings also interpret the molecular underpinnings of the two-hit scenario: the first hit is necessary for the nuclear translocation of MRTF (e.g., via Rho and

Rac activation), whereas the second one is required for MRTF activation, e.g., by eliminating an inhibiting factor. In addition, the second hit may lengthen the nuclear stay of MRTF. This view can also explain individual differences among the applied experimental systems: if MRTF is constitutively nuclear (Elberg et al., 2008), one hit (TGF-β) is likely sufficient. Alternatively, in certain cells, TGF-β may trigger strong enough Rho and/or Rac activation (Bhowmick et al., 2001) and consequent MRTF translocation, and thus, it may bring about both requirements. However, fully intact epithelia or other confluent cells are relatively insusceptible to the myogenic action of TGF-β (Masur et al., 1996; Petridou et al., 2000; Masszi et al., 2004; Fan et al., 2007). This observation has major relevance to real pathological conditions and implies that tissue injury, which can activate Rho GTPases either by uncoupling intercellular contacts (Fan et al., 2007; Samarin et al., 2007; Busche et al., 2008; Sebe et al., 2008) and/or by integrin stimulation (Chen et al., 2006; Kim et al., 2009b), may hugely potentiate the SMA-inducing effect of TGF-β. This in turn may lead to dysregulated epithelial healing and excessive MF differentiation.

In skeletal muscle, Smads have been shown to suppress myogenesis (Liu et al., 2001; Zhu et al., 2004). Recently, an interesting mechanism has been proposed whereby a complex

between MRTF-A and Smad 1/4 may inhibit skeletal muscle differentiation in a CArG-independent manner by inducing the expression of the Id3 (inhibitor of differention-3) protein (Iwasaki et al., 2008). Id3 is an antagonist of basic helix-loop-helix transcription factors, which target E boxes present in the promoter of many muscle genes, including SMA. Although such mechanisms may also operate in the epithelium, the Smad3-mediated inhibition of the MRTF-induced activation of the SMA promoter clearly represents a distinct mode of regulation. This is evident from our finding that the inhibitory action of Smad3 against MRTF is manifest in a short promoter construct, which does not contain E boxes.

We identified a 7-aa segment within the B1 region of MRTF-B, which is critical both for the MRTF–Smad3 binding and for the efficient inhibition of the MRTF-triggered SMA promoter by Smad3. The simplest interpretation of our data is that direct binding between Smad3 and MRTF inhibits the interaction between MRTF and the CArG box–SRF complex (Fig. 9 A). Consistent with such mechanism (a), the binding sites for Smad3 and SRF on MRTF are adjacent, (b) the MRTF–SRF association inversely correlates with Smad3 expression (Fig. 7), and (c) Smad3 down-regulation enhances MRTF binding to the CArG boxes of the endogenous SMA promoter (Fig. 5). A possible additional mechanism invokes that SRF can directly bind to Smad3 (Lee et al., 2007), which may also inhibit the SRF–MRTF association (Fig. 9).

The interaction of MRTF or myocardin with Smad3 has multiple functional consequences. The MRTF–Smad3 complex has been implicated in the down-regulation of E-cadherin by inducing its negative regulator, Slug, through a nonconventional SBE (Morita et al., 2007a). This way, the MRTF–Smad3 complex facilitates the loss of epithelial characteristics, i.e., the first phase of EMT. Interestingly, in fibroblasts, Smad3 was found to increase the activity of myocardin or SRF on some smooth muscle–related promoters in a CArG-independent manner (Qiu et al., 2005). It remains to be tested whether such an effect is specific to myocardin as opposed to MRTF and/or to fibroblasts. In any case, our results show that the inhibitory action of Smad3 on MRTF-mediated, CArG-dependent SMA transcription vastly overrules any potential CArG-independent stimulatory effect during EMyT. Finally, SRF binding to Smad3 can also antagonize SBE-mediated TGF-β effects, e.g., apoptosis (Lee et al., 2007). In summary, bilateral and mutually competitive interactions between the vertices of the MRTF–Smad3–SRF triangle may determine the dominant features and timing of the various phases of EMyT (Fig. 9 A). The interaction of MRTF with Smad3 may help suppress the epithelial markers, and at the same time, it puts SMA expression and MF transition on hold by competing with the SRF–MRTF interaction. Once Smad3 is degraded, the MRTF–SRF complex will dominate and lead to myogenic reprogramming.
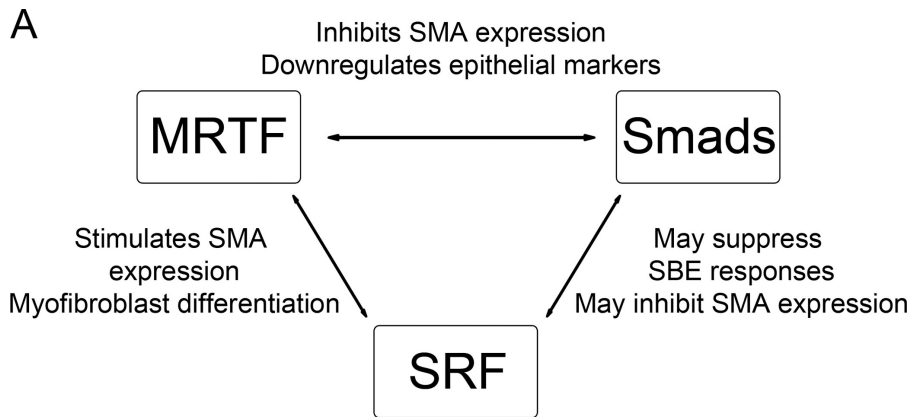
We show that both transcriptional and posttranscriptional mechanisms contribute to the two hit–induced reduction in Smad3 levels (Fig. 4). Consistent with this, TGF-β was reported to suppress Smad3 mRNA transcription (Yanagisawa et al., 1998), whereas phosphorylation of Smad3 in its linker region by various kinases (Guo et al., 2008a,b) has been pro-

posed to promote its ubiquitination and proteasomal degradation. Future work should determine the exact mechanisms whereby TGF-β reduces Smad3 mRNA and LCM promotes Smad3 degradation.

The overall role of Smad3 in fibrogenesis and EMT (particularly in EMyT) is complex and controversial. In this study, we will consider the reported negative and positive effects. Accumulating evidence shows that the progression of fibrosis is associated with the down-regulation of R-Smad expression. In cellular and animal models of kidney (Poncelet et al., 2007) and lung (Zhao and Geverd, 2002) fibrosis (which involve EMT), Smad3 levels dropped dramatically, and this process was concomitant with SMA expression. Decreased Smad2 levels and increased expression of Smad ubiquitination regulatory factor-2 were reported in animal models and patients with fibrogenic nephropathies (Tan et al., 2008). Furthermore, reduced Smad3 phosphorylation and nuclear translocation were observed during MF formation in skin and liver (Dooley et al., 2001; Reisdorf et al., 2001). Although these studies showed that the progression of fibrosis and R-Smad down-regulation occur in parallel, it remained unknown whether there is a cause–effect relationship between these events. The inhibition of MRTF by Smad3 offers a new mechanism that links these phenomena. Other compelling data connecting the loss of R-Smads with EMT come from studies on the tumor-promoting action of TGF-β. In epithelial cells expressing oncogenic mutations of the Raf–MAPK pathway, TGF-β induced EMT and loss of Smad3, whereas the reexpression of Smad3 restored the epithelial phenotype (Nicolás et al., 2003). Moreover, ablation of Smad2 in keratinocytes promoted EMT and carcinogenesis (Hoot et al., 2008). Considered together, these studies and our findings indicate that R-Smads can act as negative regulators of EMT or EMyT during fibrosis progression or tumorigenesis.

However, substantial literature suggests that R-Smads are key mediators in TGF-β–induced fibrosis and EMT (Roberts et al., 2006). Strong support for this view originates from studies using Smad3 knockout mice (Yang et al., 1999), which exhibit reduced susceptibility to matrix deposition and EMT in models of skin (Flanders et al., 2003), lens (Saika et al., 2004), and kidney fibrosis (Sato et al., 2003). However, two important points should be considered. First, much of the protection was attributed to impaired recruitment of TGF-β production by macrophages in some (Ashcroft et al., 1999), albeit not all (Lakos et al., 2004), fibrosis models in Smad3$^{-/-}$ mice. Second, Smad3 protein may not be fully eliminated from these animals. They harbor an exon 8 deletion, leading to the loss of the last 89 aa of Smad3, which leads to a functional null mutant. However, the truncated protein may be expressed (at various levels) in different tissues (Yang et al., 1999), and it may still interact with various partners, as indicated by the fact that it exerts a dominant-negative effect. Thus, the mutant may lose its profibrogenic but may keep its antifibrogenic potential. Moreover, the pathology of two Smad3 knockout mice (with either exon 2 or 8 deleted) is completely different: the first succumbs to intestinal tumors (Zhu et al., 1998) and the other to autoimmunity (Yang et al., 1999), implying the differential functional repertoire of the truncated proteins. Nonetheless, there is no

A

MRTF ⟷ Smads

Inhibits SMA expression
Downregulates epithelial markers

Stimulates SMA
expression
Myofibroblast differentiation

May suppress
SBE responses
May inhibit SMA expression

SRF

B

EMT/EMyT	
Smad phase	Non-Smad phase
Smad/MRTF collaboration	MRTF liberation
Loss of epithelial markers Gain of mesenchymal markers Expression of muscle characteristics on hold	Gain of muscle markers Motility, migration, invasiveness Cytoskeletal adaptation to MF lifestyle

Markers
Relative expression levels

Myogenic (e.g. SMA)

Mesenchymal (e.g. PAI-1)

Epithelial (e.g. E-cadherin)

Time

Figure 9. **Smad3 is a critical delayer/timer of the MF commitment in epithelial cells.** (A) Potential or tested consequences of various bilateral interactions among Smad3, MRTF, and SRF. (B) New model dissecting the process of EMyT into a Smad3-dependent (early/mesenchymal) and -independent/inhibited (late/myogenic) phase, and the proposed role of the Smad3–MRTF interaction or the lack thereof in various key events of EMyT.
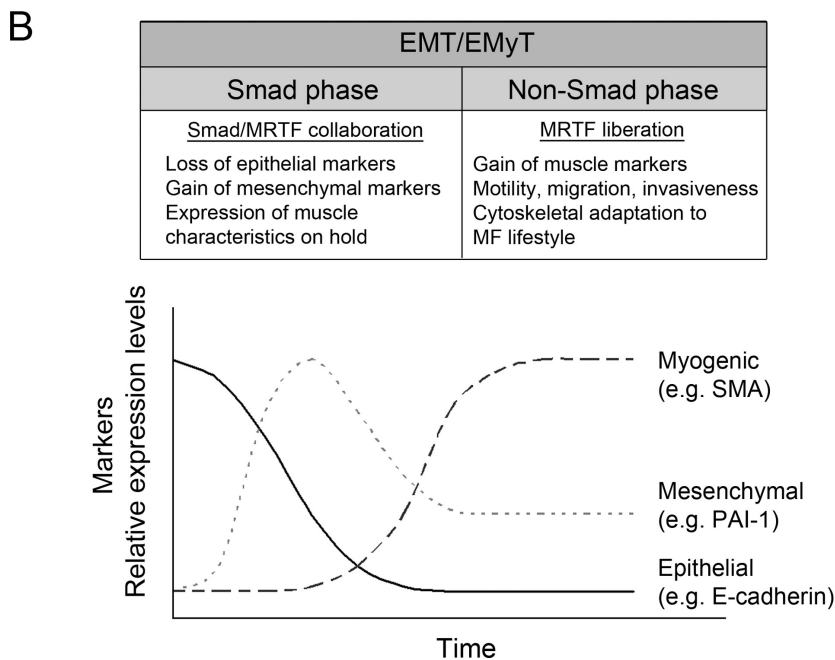
doubt that Smad3 can suppress epithelial genes (Morita et al., 2007a) and is essential for the expression of various mesenchymal genes (Massagué et al., 2005). How can these apparently disparate views be reconciled? We propose that the solution may lie in the dynamics of the process. According to our model (Fig. 9 B), EMyT can be divided into a Smad3-dependent (early/mesenchymal) and -independent (late/myogenic) phase. Smad3 contributes to the loss of epithelial markers and is critical for the expression of mesenchymal markers and certain matrix proteins. It may also prepare the second phase by promoting nuclear MRTF accumulation and the synthesis of proteins (e.g., ED-A fibronectin) that enhance SMA expression (Isono et al., 2002). This phase is followed by gradual degradation of Smad3, which enables the mobilization of the myogenic program. This switch is a prerequisite for the motile and contractile phenotype. This interpretation is also consistent with the existence of Smad3-independent EMT (Banh et al., 2006). However, in the absence of Smad3, the EMT program is diverted to a predominantly myogenic path.

In summary, we propose that Smad3 is a critical checkpoint protein or timer, which regulates (delays) the final commitment to MF transition. Clearly, future studies should test this idea in the real pathological settings of fibrotic diseases. This scenario may also provide important insights with regards to the potential benefits and problems of antifibrotic therapies aimed at the reduction of Smad3 function or expression.

Materials and methods

Reagents
The rabbit polyclonal anti-MRTF (anti-BSAC) antibody was described previously (Sasazuki et al., 2002). In whole cell lysates of LLC-PK1 cells, this antibody visualizes a doublet at ~160 kD (Sebe et al., 2008), of which the top one is more prominent in nuclear extracts. Commercially available antibodies were used against the following antigens: Flag (clone M2), SMA (clone 1A4), α-actinin (clone BM-75.2), tubulin (Sigma-Aldrich), cofilin, Smad2, phospho-Smad3, Smad4 (Cell Signaling Technology), c-Myc (clone 9E10), SRF, CTGF (Santa Cruz Biotechnology, Inc.), GAPDH (EMD), histones, α1-integrin, paxillin (Millipore), PAI-1, Smad3 (Abcam), FAK, zonula occludens-1, phospho-FAK (Invitrogen), E-cadherin and filamin A (clone 5/ABP280; BD), HA.11 (clone 16B12; Covance), and CapZ (AbD Serotec). Secondary antibodies were obtained from Jackson Immuno-Research Laboratories. Recombinant human TGF-β was obtained from R&D Systems. Rhodamine-conjugated phalloidin was obtained from Invitrogen.

Cell culture and treatment
LLC-PK1 (Cl4) cells, a porcine proximal tubular epithelial cell line (provided by R.C. Harris, Vanderbilt University School of Medicine, Nashville, TN)

were cultured in low glucose DME (Invitrogen) supplemented with 10% fetal bovine serum and 1% streptomycin/penicillin solution (Invitrogen) at 37°C in humidified atmosphere (air/CO$_2$ ratio 19:1) as in our previous study (Masszi et al., 2003). The cells were incubated under serum-free conditions for at least 3 h before various treatments. To induce cell contact disassembly, cells were thoroughly washed with PBS (Invitrogen) and cultured in nominally calcium chloride–free DME (LCM; Invitrogen). Such treatment resulted in an instant drop in transepithelial resistance measured by voltohmmeter and the disruption of cell contacts observed by phase-contrast microscopy in ∼15 min. Where indicated, cells were treated with TGF-β (4 ng/ml for biochemical experiments and 10 ng/ml for promoter luciferase assays). Human gingival fibroblasts (Pender and McCulloch, 1991) were provided by C. McCulloch (University of Toronto, Toronto, Ontario, Canada), and BEAS-2B were purchased from American Type Culture Collection.

Plasmids and transient transfection

The p765-SMA-Luc reporter construct containing the proximal 765-bp portion of the rat SMA promoter in a pGL3-basic vector (WT), the constructs harboring inactivating mutation at the SBE1 or SBE2 sites (SBE1mut and SBE2mut; Hu et al., 2003), and the p152-SMA-Luc reporter construct with the 152-bp-long SMA promoter piece were provided by S.H. Phan (University of Michigan Medical School, Ann Arbor, MI). To generate additional (or combined) mutations in certain cis-regulatory elements, PCR-based mutagenesis was performed. The mutations (in parentheses) and the corresponding primer pairs were as follows: to inactivate SBE1 (C^{-524}/T, A^{-525}/C, and C^{-528}/A), 5′-TACAGACTTCATTGATACTACA-CAAAGCTTCCAGACTACATAC-3′ and 5′-GTATGTAGTCTGGAAGCTTT-GTGTAGTATCAATGAAGTCT-3′; to mutate SBE2 (C^{+15}/T, A^{+16}/G, and G^{+17}/C), 5′-CCACCCACCTGCAGTGGAGAAGCCCAGC-3′ and 5′-CTG-GGCTTCTCCACTGCAGGTGGGTGGT-3′ (Hu et al., 2003); to mutate TCE (T^{-53}/C, G^{-52}/T, and G^{-50}/C), 5′-TGGGAAGCGAGCTGCAGGGGAT-CAGACCA-3′ and 5′-TGGTCTGATCCCCTGCAGCTCGCTTCCCA-3′ (Hu et al., 2007); to inactivate CArG-A (C^{-71}/A, C^{-70}/A, G^{-63}/A, and G^{-62}/A), 5′-CAGCCTGTCTTTGCTAATTGTTTAAGAAGCGAGTGGGAGG-3′ and 5′-CCTCCCACTCGCTTCTTAAACAATTAGCAAAGACAGGCTG-3′; and to mutate CArG-B (C^{-121}/A, C^{-120}/A, G^{-113}/A, and G^{-112}/A), 5′-GTT-TTGTGCTGAGGTAACTATATAATTGTGTTAGAGTGAACG-3′ and 5′-CGT-TCACTCTAACACAATTATATAGTTACCTCAGCACAAAAC-3′ (Shimizu et al., 1995).

These mutations were shown to effectively block the function of the corresponding cis-elements: binding of Smad3 to the mutated SBE1 or SBE2 (Hu et al., 2003) was abolished, and the TCE lost its transcriptional activity (Hu et al., 2007). The Smad3-responsive reporter construct SBE4-Luc was provided by A.B. Roberts (National Institutes of Health, Bethesda, MD). The thymidine kinase minimal promoter–driven renilla luciferase internal control plasmid, pRL-TK, was purchased from Promega. The N-terminally Myc-tagged human Smad2 and the N-terminally Myc- or Flag-tagged Smad3 expression constructs (all in pCMV5B backbone) were provided by L. Attisano (University of Toronto). From the Myc-Smad3 construct, N- (aa 1–210) and C-terminal (aa 211–405) expression constructs were generated. The Flag-tagged MRTF-B plasmid was provided by E.N. Olson (University of Texas Southwestern Medical Center, Dallas, TX). Expression of this construct in LLC-PK1 cells gives two Flag-positive bands at 160 and 110 kD. C-terminally Myc-tagged MRTF-B was generated by using the Flag- tagged MRTF-B as the template, and the MRTF sequence was cloned in frame into the Xho1–Apa1 sites of pcDNA3.1/Myc-His A. The entire construct was verified by sequencing. HA–MRTF-B was generated by engineering a double-HA tag at the N terminus of MRTF-B using standard PCR methodology. The construct was verified by sequencing. B1 region deletion mutations of HA-tagged MRTF-B were generated using primer pairs complementary to regions upstream and downstream of the specific deletion. Final constructs contained either a 7– (S279-P285; inclusive) or 13-aa deletion (S279-K291; inclusive). PCR reactions were performed using Pfu Turbo (Agilent Technologies). Resulting products were digested with Dpn1 endonuclease, transformed, and colonies were screened by restriction digest analysis or using PCR primers flanking the deletions. Selected clones were verified by sequencing. The pCGN-SRF plasmid encoding for the HA-tagged human SRF was generated by R. Prywes (Johansen and Prywes, 1993). Cells were transfected using FuGENE 6 or Lipofectamine 2000 reagents. For immunoprecipitation of heterologously expressed proteins, cells grown on 10-cm dishes were transfected with 5 µg Flag–MRTF-B and 1 µg Myc-Smad3 vectors 48 h before the experiments. In triple transfection experiments, cells grown on 10-cm dishes were transfected with 4 µg Myc-MRTF, 4 µg HA-SRF, and 6 µg Flag-Smad3 vectors for 24 h.

Luciferase reporter assays

Luciferase reporter assays were performed as described in our previous studies (Masszi et al., 2003, 2004). In brief, cells were plated onto 6-well plates and at ∼60% confluence were transfected with the mixture of 0.5 µg/well luciferase construct, 0.05 µg/well pRL-TK, and 2 µg/well empty carrier or expression vector. 16 h later, cells were serum starved for 3 h and treated for 24 h if not indicated otherwise. Finally, cells were lysed, and luciferase activity was determined using the Dual Luciferase Reporter Assay System kit (Promega) and a luminometer (Lumat 9507; Berthold) according to the manufacturers' instructions. For each condition, treatments were performed in duplicates, and experiments were repeated at least three times. From each sample, the firefly luciferase activity corresponding to a specific promoter construct was normalized to the renilla luciferase activity of the same sample. Results are expressed as fold changes compared with the mean firefly/renilla ratio of the untreated controls taken as a unit.

RNA interference

MRTF siRNAs were generated after obtaining a partial sequence of the porcine MRTF gene from LLC-PK1 cells. It is noteworthy that the sequence obtained through RT-PCR was highly homologous to MRTF-B but not to MRTF-A, suggesting that the former is the predominant and potentially the only isoform expressed in these cells. The optimal target sequences (5′-AAC-ATGGAGTGGCTAGACATT-3′ and 5′-AACAGCAGTGAAGATAGAGAG-3′) were determined using the siRNA Target Finder program (Applied Biosystems). The siRNAs against the pig Smad3 (target sequence 5′-AAG-AGTTCACTCCACATTCTC-3′; based on GenBank sequence accession no. NM_214137.1) and Smad2 (target sequence 5′-AAATACGATAGATCA-GTGGGA-3′; GenBank accession no. NW_001885794.1) and the human Smad3 (target sequence 5′-AAGGCCATCACCACGCAGAAC-3′; NM_005902.3) were designed using Target Finder tool (Applied Biosystems). NR control siRNA was purchased from Ambion. LLC-PK1 cells were cultured in antibiotic-free growth medium and transfected with 100 nM siRNA using Lipofectamine RNAiMAX (Invitrogen). For EMyT induction, cells were transfected at 60% confluence. After overnight incubation, cells reached complete confluence and were treated with the appropriate conditions of the two-hit model for 48 h.

Western blotting

After treatments, cells were scraped into Triton lysis buffer (30 mM Hepes, pH 7.4, 100 mM NaCl, 1 mM EGTA, 20 mM NaF, and 1% Triton X-100) supplemented with 1 mM Na$_3$VO$_4$, 1 mM phenylmethylsulphonyl fluoride, and Complete Mini protease inhibitor cocktail (Roche). Protein concentration was determined, and samples were denatured by boiling in Laemmli sample buffer (Bio-Rad Laboratories). Equal amount of protein (10 µg) was subjected to SDS-PAGE and Western blotting as described previously (Masszi et al., 2004). Densitometry was performed with a densitometer (GS800; Bio-Rad Laboratories) and the Quantity One software (Bio-Rad Laboratories).

Protein determination

The protein concentration from nondenatured cell lysates was determined using a BCA protein assay (Thermo Fisher Scientific) with a bovine serum albumin as standard.

Immunoprecipitation

Cells were grown on 10-cm Petri dishes, and after appropriate treatment, lysed in Triton lysis buffer. To remove cell debris, samples were spun at 12,000 rpm at 4°C for 10 min, and aliquots of samples for whole cell lysates were taken. Supernatants (∼1–2 mg protein) were precleared with protein G agarose beads (Thermo Fisher Scientific) and were incubated with the appropriate antibody (1 µg/sample). To capture immunocomplexes, protein G agarose beads were added to the mixture for 1 h. Subsequently, the beads were washed three times with Triton lysis buffer supplemented with 1 mM Na$_3$VO$_4$. Captured proteins were eluted into Laemmli sample buffer (Bio-Rad Laboratories) and analyzed by Western blotting.

Nuclear extraction

Nuclear extracts were prepared from confluent layers of LLC-PK1 cells grown on 6-cm dishes using the NE-PER Nuclear Extraction kit (Thermo Fisher Scientific) according to the manufacturer's recommendation. The nuclear extracts were collected, their protein concentration was determined, and samples of equal protein content (5 µg) were analyzed by Western blotting. Antihistone antibody was used to check for equal loading of nuclear proteins.

ChIP assay

Reagents for ChIP experiments were obtained from the EZ ChIP kit (Millipore), and assays were performed essentially as described by the manufacturer. LLC-PK1 cells were transfected with pig Smad3 or NR control siRNA using Lipofectamine RNAiMAX (Invitrogen). Efficiency of downregulation was confirmed by Western blotting of cell lysates prepared from matching plates to those used for ChIP assays. After down-regulation, cells were treated appropriately, cross-linked, lysed, and sheared by sonication (450 Sonifier; Branson). DNA fragments were subjected to immunoprecipitation with 5 µg rabbit polyclonal MRTF antibody, and purified DNA was extracted from the recovered complexes. For negative controls, parallel experiments were performed using normal rabbit IgG as the immunoprecipitating antibody. Input and purified DNA from each sample were analyzed by SYBR green–based real-time PCR (IQ5 cycler; Bio-Rad Laboratories) using primers to amplify a CArG-containing region of the pig SMA promoter. Primer sequences were as follows: 5′-AGTTTTGTGC-TGAGGTCCCTATATG-3′ and 5′-TTCCCAAACAAGGAACAAAGA-3′. Semi-qPCR was also performed by running products on a 3% agarose gel to detect the 79-bp amplicon.

Immunofluorescence microscopy

Cells grown on glass coverslips were fixed with 4% paraformaldehyde for 30 min followed by intensive washing with PBS and incubation with 100 mM glycine in PBS for 10 min. Cells were permeabilized in PBS containing 1% Triton X-100 and 0.5% bovine serum albumin for 20 min, blocked in 3% BSA in PBS for 1 h, and incubated with primary antibody for an additional 1 h. After a thorough wash, cells were incubated with the corresponding fluorescently labeled secondary antibody with Cy3 dye (Jackson ImmunoResearch Laboratories). To visualize cotransfected Myc- and Flag-tagged proteins simultaneously, samples were first incubated with anti-Flag (M2; Sigma-Aldrich) and Cy3-labeled anti–mouse antibodies and were stained with anti-Myc antibody (9E10) directly conjugated with FITC (Santa Cruz Biotechnology, Inc.). To visualize F-actin, fixed cells were incubated with rhodamine-labeled phalloidin (Invitrogen). For nuclear labeling, cells were stained with DAPI (Invitrogen), and coverslips were mounted on slides using fluorescent mounting medium (Dako). Samples were analyzed using a microscope (IX81; Olympus) with a UPlan S-Apo 60× 1.42 NA oil objective (Olympus) coupled to a camera (Evolution QEi Monochrome; Media Cybernetics) controlled by imaging software (QED InVivo; Media Cybernetics). Images were processed using ImagePro Plus software (3DS 5.1; Media Cybernetics) and Photoshop (CS4; Adobe). Modifications were restricted exclusively to minor adjustments of brightness/contrast. MRTF distribution was quantified as described previously (Fan et al., 2007), except even stricter criteria were used to denote MRTF as nuclear. Staining intensity was measured along a line across the cells, and the mean intensity in the cytoplasm and nucleus (verified by DAPI staining) was determined. MRTF localization was categorized as nuclear if the nuclear/cytoplasmic ratio was >1.5. This value corresponds to a clear nuclear accumulation as assessed by simple visual inspection (in unstimulated cells, the mean ratio is 0.6; i.e., there is a clear nuclear exclusion). Slides were evaluated by two independent observers, and at least 10 randomly selected fields (>200 cells) were quantified for each condition in three experiments.

mRNA analysis

LLC-PK1 cells transfected with pig Smad3 or NR siRNA for 54 h were serum deprived for 3 h and treated with or without TGF-β or LCM for 3 or 6 h. In other experiments, nontransfected cells were exposed for 24 h to the four conditions of the two-hit scheme. After these treatments, RNA was extracted using an RNeasy kit (QIAGEN), and cDNA was synthesized from 1 µg total RNA using iScript reverse transcription (Bio-Rad Laboratories). SYBR green–based real-time PCR was used to evaluate gene expression of PAI-1, SMA, and Smad3 using GAPDH as an endogenous control. Primer pairs designed against known pig sequences were used as follows: SMA, 5′-TGTGACAATGGTTCTGGGCTCTGT-3′ and 5′-TTCGTCACCCAC-GTAGCTGTCTTT-3′; Smad3, 5′-GCAGAACGTCAACACCAAGTGCAT-3′ and 5′-ATTCACGCAGACCTCGTCCTTCTT-3′; PAI-1, 5′-CCACTGCTCT-GGTGGTGAGA-3′ and 5′-GTTCTCGATGGTGGTGCTTT-3′; GAPDH, 5′-GCAAAGTGGACATGGTCGCCATCA-3′ and 5′-AGCTTCCCATTCT-CAGCCTTGACT-3′. Products from semi-qPCR were analyzed on 2% agarose gels.

Statistical analysis

Data are presented as blots or images from at least three similar experiments or as the means ± SEM for the number of experiments indicated. Statistical significance was determined by Student's *t* test or one-way analy-sis of variance (Tukey posthoc testing) as appropriate using Prism software (version 4.0; GraphPad Software, Inc.). $P < 0.05$ was accepted as significant and is indicated with asterisks.

Online supplemental material

Fig. S1 shows the effect of TGF-β, LCM, and their combination on the expression of a variety of cytoskeletal components regulated by CArG boxes. Using an alternative siRNA (Fig. 1 A), the results confirm that MRTF is necessary for basal expression or upregulation of these proteins. Fig. S2 depicts key controls, showing that Smad3 binds MRTF and indicates that Smad3 facilitates the nuclear accumulation of MRTF. Online supplemental material is available at http://www.jcb.org/cgi/content/full/jcb.200906155/DC1.

References

Ashcroft, G.S., X. Yang, A.B. Glick, M. Weinstein, J.L. Letterio, D.E. Mizel, M. Anzano, T. Greenwell-Wild, S.M. Wahl, C. Deng, and A.B. Roberts. 1999. Mice lacking Smad3 show accelerated wound healing and an impaired local inflammatory response. *Nat. Cell Biol.* 1:260–266. doi:10.1038/12971

Banh, A., P.A. Deschamps, J. Gauldie, P.A. Overbeek, J.G. Sivak, and J.A. West-Mays. 2006. Lens-specific expression of TGF-beta induces anterior subcapsular cataract formation in the absence of Smad3. *Invest. Ophthalmol. Vis. Sci.* 47:3450–3460. doi:10.1167/iovs.05-1208

Bhowmick, N.A., M. Ghiassi, A. Bakin, M. Aakre, C.A. Lundquist, M.E. Engel, C.L. Arteaga, and H.L. Moses. 2001. Transforming growth factor-beta1 mediates epithelial to mesenchymal transdifferentiation through a RhoA-dependent mechanism. *Mol. Biol. Cell.* 12:27–36.

Busche, S., A. Descot, S. Julien, H. Genth, and G. Posern. 2008. Epithelial cell-cell contacts regulate SRF-mediated transcription via Rac-actin-MAL signalling. *J. Cell Sci.* 121:1025–1035. doi:10.1242/jcs.014456

Chen, C.A., J.C. Hwang, J.Y. Guh, J.C. Tsai, and H.C. Chen. 2006. TGF-beta1 and integrin synergistically facilitate the differentiation of rat podocytes by increasing alpha-smooth muscle actin expression. *Transl. Res.* 148:134–141. doi:10.1016/j.trsl.2006.03.008

Dooley, S., B. Delvoux, M. Streckert, L. Bonzel, M. Stopa, P. ten Dijke, and A.M. Gressner. 2001. Transforming growth factor beta signal transduction in hepatic stellate cells via Smad2/3 phosphorylation, a pathway that is abrogated during in vitro progression to myofibroblasts. TGFbeta signal transduction during transdifferentiation of hepatic stellate cells. *FEBS Lett.* 502:4–10. doi:10.1016/S0014-5793(01)02656-4

Elberg, G., L. Chen, D. Elberg, M.D. Chan, C.J. Logan, and M.A. Turman. 2008. MKL1 mediates TGF-beta1-induced alpha-smooth muscle actin expression in human renal epithelial cells. *Am. J. Physiol. Renal Physiol.* 294:F1116–F1128. doi:10.1152/ajprenal.00142.2007

Fan, L., A. Sebe, Z. Péterfi, A. Masszi, A.C. Thirone, O.D. Rotstein, H. Nakano, C.A. McCulloch, K. Szászi, I. Mucsi, and A. Kapus. 2007. Cell contact-dependent regulation of epithelial-myofibroblast transition via the rho-rho kinase-phospho-myosin pathway. *Mol. Biol. Cell.* 18:1083–1097. doi:10.1091/mbc.E06-07-0602

Flanders, K.C., C.D. Major, A. Arabshahi, E.E. Aburime, M.H. Okada, M. Fujii, T.D. Blalock, G.S. Schultz, A. Sowers, M.A. Anzano, et al. 2003. Interference with transforming growth factor-beta/ Smad3 signaling results in accelerated healing of wounds in previously irradiated skin. *Am. J. Pathol.* 163:2247–2257.

Guo, X., A. Ramirez, D.S. Waddell, Z. Li, X. Liu, and X.F. Wang. 2008a. Axin and GSK3- control Smad3 protein stability and modulate TGF- signaling. *Genes Dev.* 22:106–120. doi:10.1101/gad.1590908

Guo, X., D.S. Waddell, W. Wang, Z. Wang, N.T. Liberati, S. Yong, X. Liu, and X.F. Wang. 2008b. Ligand-dependent ubiquitination of Smad3 is regulated by casein kinase 1 gamma 2, an inhibitor of TGF-beta signaling. *Oncogene.* 27:7235–7247. doi:10.1038/onc.2008.337

Hautmann, M.B., P.J. Adam, and G.K. Owens. 1999. Similarities and differences in smooth muscle alpha-actin induction by TGF-beta in smooth muscle versus non-smooth muscle cells. *Arterioscler. Thromb. Vasc. Biol.* 19:2049–2058.

Hill, C.S., J. Wynne, and R. Treisman. 1995. The Rho family GTPases RhoA, Rac1, and CDC42Hs regulate transcriptional activation by SRF. *Cell.* 81:1159–1170. doi:10.1016/S0092-8674(05)80020-0

Hoot, K.E., J. Lighthall, G. Han, S.L. Lu, A. Li, W. Ju, M. Kulesz-Martin, E. Bottinger, and X.J. Wang. 2008. Keratinocyte-specific Smad2 ablation results in increased epithelial-mesenchymal transition during skin cancer formation and progression. *J. Clin. Invest.* 118:2722–2732.

Hu, B., Z. Wu, and S.H. Phan. 2003. Smad3 mediates transforming growth factor-beta-induced alpha-smooth muscle actin expression. *Am. J. Respir. Cell Mol. Biol.* 29:397–404. doi:10.1165/rcmb.2003-0063OC

Hu, B., Z. Wu, T. Liu, M.R. Ullenbruch, H. Jin, and S.H. Phan. 2007. Gut-enriched Krüppel-like factor interaction with Smad3 inhibits myofibroblast differentiation. *Am. J. Respir. Cell Mol. Biol.* 36:78–84. doi:10.1165/rcmb.2006-0043OC

Isono, M., S. Chen, S.W. Hong, M.C. Iglesias-de la Cruz, and F.N. Ziyadeh. 2002. Smad pathway is activated in the diabetic mouse kidney and Smad3 mediates TGF-beta-induced fibronectin in mesangial cells. *Biochem. Biophys. Res. Commun.* 296:1356–1365. doi:10.1016/S0006-291X(02)02084-3

Iwano, M., D. Plieth, T.M. Danoff, C. Xue, H. Okada, and E.G. Neilson. 2002. Evidence that fibroblasts derive from epithelium during tissue fibrosis. *J. Clin. Invest.* 110:341–350.

Iwasaki, K., K. Hayashi, T. Fujioka, and K. Sobue. 2008. Rho/Rho-associated kinase signal regulates myogenic differentiation via myocardin-related transcription factor-A/Smad-dependent transcription of the Id3 gene. *J. Biol. Chem.* 283:21230–21241. doi:10.1074/jbc.M710525200

Johansen, F.E., and R. Prywes. 1993. Identification of transcriptional activation and inhibitory domains in serum response factor (SRF) by using GAL4-SRF constructs. *Mol. Cell. Biol.* 13:4640–4647.

Kalluri, R., and E.G. Neilson. 2003. Epithelial-mesenchymal transition and its implications for fibrosis. *J. Clin. Invest.* 112:1776–1784.

Kim, K.K., M.C. Kugler, P.J. Wolters, L. Robillard, M.G. Galvez, A.N. Brumwell, D. Sheppard, and H.A. Chapman. 2006. Alveolar epithelial cell mesenchymal transition develops in vivo during pulmonary fibrosis and is regulated by the extracellular matrix. *Proc. Natl. Acad. Sci. USA.* 103:13180–13185. doi:10.1073/pnas.0605669103

Kim, K.K., Y. Wei, C. Szekeres, M.C. Kugler, P.J. Wolters, M.L. Hill, J.A. Frank, A.N. Brumwell, S.E. Wheeler, J.A. Kreidberg, and H.A. Chapman. 2009a. Epithelial cell alpha3beta1 integrin links beta-catenin and Smad signaling to promote myofibroblast formation and pulmonary fibrosis. *J. Clin. Invest.* 119:213–224.

Kim, Y., M.C. Kugler, Y. Wei, K.K. Kim, X. Li, A.N. Brumwell, and H.A. Chapman. 2009b. Integrin α3β1-dependent β-catenin phosphorylation links epithelial Smad signaling to cell contacts. *J. Cell Biol.* 184:309–322. doi:10.1083/jcb.200806067

Klymkowsky, M.W., and P. Savagner. 2009. Epithelial-mesenchymal transition: a cancer researcher's conceptual friend and foe. *Am. J. Pathol.* 174:1588–1593. doi:10.2353/ajpath.2009.080545

Lakos, G., S. Takagawa, S.J. Chen, A.M. Ferreira, G. Han, K. Masuda, X.J. Wang, L.A. DiPietro, and J. Varga. 2004. Targeted disruption of TGF-beta/Smad3 signaling modulates skin fibrosis in a mouse model of scleroderma. *Am. J. Pathol.* 165:203–217.

Lee, J.M., S. Dedhar, R. Kalluri, and E.W. Thompson. 2006. The epithelial–mesenchymal transition: new insights in signaling, development, and disease. *J. Cell Biol.* 172:973–981. doi:10.1083/jcb.200601018

Lee, H.J., C.H. Yun, S.H. Lim, B.C. Kim, K.G. Baik, J.M. Kim, W.H. Kim, and S.J. Kim. 2007. SRF is a nuclear repressor of Smad3-mediated TGF-beta signaling. *Oncogene.* 26:173–185. doi:10.1038/sj.onc.1209774

Liu, D., B.L. Black, and R. Derynck. 2001. TGF-beta inhibits muscle differentiation through functional repression of myogenic transcription factors by Smad3. *Genes Dev.* 15:2950–2966. doi:10.1101/gad.925901

Liu, Y., S. Sinha, O.G. McDonald, Y. Shang, M.H. Hoofnagle, and G.K. Owens. 2005. Kruppel-like factor 4 abrogates myocardin-induced activation of smooth muscle gene expression. *J. Biol. Chem.* 280:9719–9727. doi:10.1074/jbc.M412862200

Massagué, J., J. Seoane, and D. Wotton. 2005. Smad transcription factors. *Genes Dev.* 19:2783–2810. doi:10.1101/gad.1350705

Masszi, A., C. Di Ciano, G. Sirokmány, W.T. Arthur, O.D. Rotstein, J. Wang, C.A. McCulloch, L. Rosivall, I. Mucsi, and A. Kapus. 2003. Central role for Rho in TGF-beta1-induced alpha-smooth muscle actin expression during epithelial-mesenchymal transition. *Am. J. Physiol. Renal Physiol.* 284:F911–F924.

Masszi, A., L. Fan, L. Rosivall, C.A. McCulloch, O.D. Rotstein, I. Mucsi, and A. Kapus. 2004. Integrity of cell-cell contacts is a critical regulator of TGF-beta 1-induced epithelial-to-myofibroblast transition: role for beta-catenin. *Am. J. Pathol.* 165:1955–1967.

Masur, S.K., H.S. Dewal, T.T. Dinh, I. Erenburg, and S. Petridou. 1996. Myofibroblasts differentiate from fibroblasts when plated at low density. *Proc. Natl. Acad. Sci. USA.* 93:4219–4223. doi:10.1073/pnas.93.9.4219

Miano, J.M., X. Long, and K. Fujiwara. 2007. Serum response factor: master regulator of the actin cytoskeleton and contractile apparatus. *Am. J. Physiol. Cell Physiol.* 292:C70–C81. doi:10.1152/ajpcell.00386.2006

Miralles, F., G. Posern, A.I. Zaromytidou, and R. Treisman. 2003. Actin dynamics control SRF activity by regulation of its coactivator MAL. *Cell.* 113:329–342. doi:10.1016/S0092-8674(03)00278-2

Morita, T., T. Mayanagi, and K. Sobue. 2007a. Dual roles of myocardin-related transcription factors in epithelial–mesenchymal transition via *slug* induction and actin remodeling. *J. Cell Biol.* 179:1027–1042. doi:10.1083/jcb.200708174

Morita, T., T. Mayanagi, and K. Sobue. 2007b. Reorganization of the actin cytoskeleton via transcriptional regulation of cytoskeletal/focal adhesion genes by myocardin-related transcription factors (MRTFs/MAL/MKLs). *Exp. Cell Res.* 313:3432–3445. doi:10.1016/j.yexcr.2007.07.008

Nakaya, Y., and G. Sheng. 2008. Epithelial to mesenchymal transition during gastrulation: an embryological view. *Dev. Growth Differ.* 50:755–766.

Nicolás, F.J., K. Lehmann, P.H. Warne, C.S. Hill, and I. Downward. 2003. Epithelial to mesenchymal transition in Madin-Darby canine kidney cells is accompanied by down-regulation of Smad3 expression, leading to resistance to transforming growth factor-beta-induced growth arrest. *J. Biol. Chem.* 278:3251–3256. doi:10.1074/jbc.M209019200

Pender, N., and C.A. McCulloch. 1991. Quantitation of actin polymerization in two human fibroblast sub-types responding to mechanical stretching. *J. Cell Sci.* 100:187–193.

Petridou, S., O. Maltseva, S. Spanakis, and S.K. Masur. 2000. TGF-beta receptor expression and smad2 localization are cell density dependent in fibroblasts. *Invest. Ophthalmol. Vis. Sci.* 41:89–95.

Poncelet, A.C., H.W. Schnaper, R. Tan, Y. Liu, and C.E. Runyan. 2007. Cell phenotype-specific down-regulation of Smad3 involves decreased gene activation as well as protein degradation. *J. Biol. Chem.* 282:15534–15540. doi:10.1074/jbc.M701991200

Posern, G., and R. Treisman. 2006. Actin' together: serum response factor, its cofactors and the link to signal transduction. *Trends Cell Biol.* 16:588–596. doi:10.1016/j.tcb.2006.09.008

Qiu, P., X.H. Feng, and L. Li. 2003. Interaction of Smad3 and SRF-associated complex mediates TGF-beta1 signals to regulate SM22 transcription during myofibroblast differentiation. *J. Mol. Cell. Cardiol.* 35:1407–1420. doi:10.1016/j.yjmcc.2003.09.002

Qiu, P., R.P. Ritchie, Z. Fu, D. Cao, J. Cumming, J.M. Miano, D.Z. Wang, H.J. Li, and L. Li. 2005. Myocardin enhances Smad3-mediated transforming growth factor-beta1 signaling in a CArG box-independent manner: Smad-binding element is an important cis element for SM22alpha transcription in vivo. *Circ. Res.* 97:983–991. doi:10.1161/01.RES.0000190604.90049.71

Reisdorf, P., D.A. Lawrence, V. Sivan, E. Klising, and M.T. Martin. 2001. Alteration of transforming growth factor-beta1 response involves down-regulation of Smad3 signaling in myofibroblasts from skin fibrosis. *Am. J. Pathol.* 159:263–272.

Roberts, A.B., F. Tian, S.D. Byfield, C. Stuelten, A. Ooshima, S. Saika, and K.C. Flanders. 2006. Smad3 is key to TGF-beta-mediated epithelial-to-mesenchymal transition, fibrosis, tumor suppression and metastasis. *Cytokine Growth Factor Rev.* 17:19–27. doi:10.1016/j.cytogfr.2005.09.008

Saika, S., S. Kono-Saika, Y. Ohnishi, M. Sato, Y. Muragaki, A. Ooshima, K.C. Flanders, J. Yoo, M. Anzano, C.Y. Liu, et al. 2004. Smad3 signaling is required for epithelial-mesenchymal transition of lens epithelium after injury. *Am. J. Pathol.* 164:651–663.

Samarin, S.N., A.I. Ivanov, G. Flatau, C.A. Parkos, and A. Nusrat. 2007. Rho/ROCK-II signaling mediates disassembly of epithelial apical junctions. *Mol. Biol. Cell.* 18:3429–3439. doi:10.1091/mbc.E07-04-0315

Sasazuki, T., T. Sawada, S. Sakon, T. Kitamura, T. Kishi, T. Okazaki, M. Katano, M. Tanaka, M. Watanabe, H. Yagita, et al. 2002. Identification of a novel transcriptional activator, BSAC, by a functional cloning to inhibit tumor necrosis factor-induced cell death. *J. Biol. Chem.* 277:28853–28860. doi:10.1074/jbc.M203190200

Sato, M., Y. Muragaki, S. Saika, A.B. Roberts, and A. Ooshima. 2003. Targeted disruption of TGF-beta1/Smad3 signaling protects against renal tubulo-interstitial fibrosis induced by unilateral ureteral obstruction. *J. Clin. Invest.* 112:1486–1494.

Sebe, A., A. Masszi, M. Zulys, T. Yeung, P. Speight, O.D. Rotstein, H. Nakano, I. Mucsi, K. Szászi, and A. Kapus. 2008. Rac, PAK and p38 regulate cell contact-dependent nuclear translocation of myocardin-related transcription factor. *FEBS Lett.* 582:291–298. doi:10.1016/j.febslet.2007.12.021

Shimizu, R.T., R.S. Blank, R. Jervis, S.C. Lawrenz-Smith, and G.K. Owens. 1995. The smooth muscle alpha-actin gene promoter is differentially regulated in smooth muscle versus non-smooth muscle cells. *J. Biol. Chem.* 270:7631–7643. doi:10.1074/jbc.270.6.2460

Sun, Q., G. Chen, J.W. Streb, X. Long, Y. Yang, C.J. Stoeckert Jr., and J.M. Miano. 2006. Defining the mammalian CArGome. *Genome Res.* 16:197–207. doi:10.1101/gr.4108706

Tan, R., W. He, X. Lin, L.P. Kiss, and Y. Liu. 2008. Smad ubiquitination regulatory factor-2 in the fibrotic kidney: regulation, target specificity, and functional implication. *Am. J. Physiol. Renal Physiol.* 294:F1076–F1083. doi:10.1152/ajprenal.00323.2007

Wang, D., P.S. Chang, Z. Wang, L. Sutherland, J.A. Richardson, E. Small, P.A. Krieg, and E.N. Olson. 2001. Activation of cardiac gene expression by myocardin, a transcriptional cofactor for serum response factor. *Cell.* 105:851–862. doi:10.1016/S0092-8674(01)00404-4

Wang, D.Z., S. Li, D. Hockemeyer, L. Sutherland, Z. Wang, G. Schratt, J.A. Richardson, A. Nordheim, and E.N. Olson. 2002. Potentiation of serum response factor activity by a family of myocardin-related transcription factors. *Proc. Natl. Acad. Sci. USA.* 99:14855–14860. doi:10.1073/pnas.222561499

Xu, J., S. Lamouille, and R. Derynck. 2009. TGF-beta-induced epithelial to mesenchymal transition. *Cell Res.* 19:156–172. doi:10.1038/cr.2009.5

Yanagisawa, K., H. Osada, A. Masuda, M. Kondo, T. Saito, Y. Yatabe, K. Takagi, T. Takahashi, and T. Takahashi. 1998. Induction of apoptosis by Smad3 and down-regulation of Smad3 expression in response to TGF-beta in human normal lung epithelial cells. *Oncogene.* 17:1743–1747. doi:10.1038/sj.onc.1202052

Yang, J., and Y. Liu. 2001. Dissection of key events in tubular epithelial to myofibroblast transition and its implications in renal interstitial fibrosis. *Am. J. Pathol.* 159:1465–1475.

Yang, X., J.J. Letterio, R.J. Lechleider, L. Chen, R. Hayman, H. Gu, A.B. Roberts, and C. Deng. 1999. Targeted disruption of SMAD3 results in impaired mucosal immunity and diminished T cell responsiveness to TGF-beta. *EMBO J.* 18:1280–1291. doi:10.1093/emboj/18.5.1280

Zaromytidou, A.I., F. Miralles, and R. Treisman. 2006. MAL and ternary complex factor use different mechanisms to contact a common surface on the serum response factor DNA-binding domain. *Mol. Cell. Biol.* 26:4134–4148. doi:10.1128/MCB.01902-05

Zhao, Y., and D.A. Geverd. 2002. Regulation of Smad3 expression in bleomycin-induced pulmonary fibrosis: a negative feedback loop of TGF-beta signaling. *Biochem. Biophys. Res. Commun.* 294:319–323. doi:10.1016/S0006-291X(02)00471-0

Zhu, Y., J.A. Richardson, L.F. Parada, and J.M. Graff. 1998. Smad3 mutant mice develop metastatic colorectal cancer. *Cell.* 94:703–714. doi:10.1016/S0092-8674(00)81730-4

Zhu, S., P.J. Goldschmidt-Clermont, and C. Dong. 2004. Transforming growth factor-beta-induced inhibition of myogenesis is mediated through Smad pathway and is modulated by microtubule dynamic stability. *Circ. Res.* 94:617–625. doi:10.1161/01.RES.0000118599.25944.D5